

Stephen F. Austin State University

SFA ScholarWorks

Electronic Theses and Dissertations

Spring 5-14-2016

Characterization of Lower Permian Carbonate Subaqueous Gravity Flows in Crockett County, Texas

Wesley L. Turner

Stephen F Austin State University, westurner510@gmail.com

Follow this and additional works at: <https://scholarworks.sfasu.edu/etds>



Part of the [Geology Commons](#), [Sedimentology Commons](#), and the [Stratigraphy Commons](#)

[Tell us](#) how this article helped you.

Repository Citation

Turner, Wesley L., "Characterization of Lower Permian Carbonate Subaqueous Gravity Flows in Crockett County, Texas" (2016). *Electronic Theses and Dissertations*. 44.

<https://scholarworks.sfasu.edu/etds/44>

This Thesis is brought to you for free and open access by SFA ScholarWorks. It has been accepted for inclusion in Electronic Theses and Dissertations by an authorized administrator of SFA ScholarWorks. For more information, please contact cdsscholarworks@sfasu.edu.

Characterization of Lower Permian Carbonate Subaqueous Gravity Flows in Crockett County, Texas

Creative Commons License



This work is licensed under a [Creative Commons Attribution-Noncommercial-No Derivative Works 4.0 License](https://creativecommons.org/licenses/by-nc-nd/4.0/).

Characterization of Lower Permian Carbonate Subaqueous Gravity Flows in
Crockett County, Texas

By

Wesley Luke Turner, Bachelors of Science

Presented to the Faculty of the Graduate School of
Stephen F. Austin State University

In Partial Fulfillment

Of the Requirements

For the Degree of

Master of Science

STEPHEN F. AUSTIN STATE UNIVERSITY

May, 2016

Characterization of Lower Permian Carbonate Subaqueous Gravity Flows in
Crockett County, Texas

By

Wesley Luke Turner, Bachelors of Science

APPROVED:

Dr. R. LaRell Nielson, Thesis Director

Dr. Wesley Brown, Committee Member

Dr. Kevin Stafford, Committee Member

Dr. Robert Friedfeld, Committee Member

Richard Berry, D.M.A.
Dean of the Graduate School

ABSTRACT

Transitional sediments on carbonate ramp slopes act as a link to relatively well-studied platform and basin depositional environments. In the southern Midland Basin, the key to understanding the relationship between these environments lies in the allochthonous gravity flow sediments found on the slope. Here, a succession of various gravity flow deposits is used to interpret how base level fluctuations affect the type of deposits found on the slope and their effect on the deep basinal environment. This study utilizes core samples from the Wolfcamp Formation adjacent to the Central Basin Platform in five wells in Northwest Crockett County, Texas. The objective is to define lithofacies, explore facies relationships, and calibrate well logs to core in order to determine how changes in sedimentation along the platform margin and slope are related to base level and slope architecture. Gamma ray, neutron density, and resistivity well logs allow the correlation of the lithologic units and the lithofacies. Interpretation of stratal stacking patterns and gravity flow transport processes are used to interpret highstands shedding of grainstones, falling stage and lowstands carbonate conglomerate debris, and a transgressive drape of shale ending a full second order sequence that takes place during the deposition of the Wolfcamp Formation.

TABLE OF CONTENTS

CHAPTER	Page
INTRODUCTION.....	1
STUDY AREA.....	3
GEOLOGIC HISTORY.....	4
LITERATURE REVIEW.....	9
Carbonate Slope Depositional Controls.....	11
PURPOSE.....	15
METHODOLOGY.....	16
STRATIGRAPHY.....	17
LITHOFACIES.....	20
Bioclast packstone to grainstone lithofacies.....	22
Porous bioclast packstone to grainstone lithofacies.....	25
Lithoclast rudstone to floatstone lithofacies.....	25
Massive to laminated shale lithofacies.....	30
Bioclast and lithoclast wackestone lithofacies.....	32
LOG FACIES AND CORE CALIBRATION.....	34
Thick-bedded log facies.....	37
Porous log facies.....	38
Thin-bedded log facies.....	39

Shale log facies.....	40
INITIATION, TRANSPORT, AND RELATIONSHIP OF GRAVITY FLOWS.....	41
DEPOSITIONAL FACIES.....	44
Turbidite facies.....	44
Grain flow facies.....	45
Debris flow facies.....	46
Stratigraphic relationships.....	47
LITHOFACIES INTERPRETATION.....	54
EXPLORATION CONSIDERATIONS.....	60
CONCLUSION.....	62
FUTURE WORK.....	64
REFERENCES.....	65
APPENDIX.....	70
VITA.....	86

LIST OF FIGURES

	Page
1. Location of study area and wells used in study with mapped Lower Wolfcamp platform edge (Hobson et al., 1985).....	2
2. Extent of Ordovician carbonate deposition along the great American carbonate bank (Sternbach, 2012)	5
3. Sub-basin configuration of the Permian basin during the Permian (Ward et al., 1986)	7
4. Stratigraphy and 2 nd order relative sea level changes in the Permian during the Lower Absaroka megasequence (Sarg et al., 1999)	8
5. Carbonate slope profiles and their mathematical expressions (Adams and Kenter, 2013)	14
6. Generalized stratigraphic column throughout the Permian (Modified from Mazullo and Reid, 1989)	18
7. Example of bioclast packstone to grainstone lithofacies in Simpson Canyon 1036	23
8. Example of bioclast packstone to grainstone lithofacies in Simpson Canyon 1046	24
9. Example of porous bioclast packstone to grainstone lithofacies in Simpson Canyon 1046	26
10. Example of porous bioclast packstone to grainstone lithofacies in Simpson Canyon 5027	27
11. Example of lithoclast rudstone to floatstone lithofacies in Simpson Canyon 4045	28
12. Example of lithoclast rudstone to floatstone lithofacies in Simpson Canyon 1036	29

13. Example of laminated to massive shale lithofacies in Simpson Canyon 5027	31
14. Example of bioclast wackestone to packstone lithofacies in Simpson Canyon 4045	33
15. Calibration of core with well log in Simpson Canyon 4045	36
16. Diagram illustrating type of resedimented carbonate gravity flow and relative distance from platform source. (Enos and Moore, 1983)	43
17. Stratigraphic cross-section along dip of the study area with well logs and position of cores	48
18. Diagram illustrating stacking patterns of debris flows from computer simulation and diagrammatic cross-section of debris flow morphology (Pratson et al., 2000; Elverhoi, 2005)	50
19. Stratigraphic cross-section along strike of the study area with well logs and position of cores	53
20. Stratigraphic column of the eastern Central Basin Platform (Saller et al., 1994)	55
A-1. Table of all wells used in study along with data type available	70
A-2. Core image of Simpson Canyon 1036 interval 6237' to 6257'	71
A-3. Core image of Simpson Canyon 1036 interval 6257' to 6279'	72
A-4. Core image of Simpson Canyon 1036 interval 6279' to 6297'	73
A-5. Core image of Simpson Canyon 1036 interval 6297' to 6216'	74
A-6. Core image of Simpson Canyon 1044 interval 5584' to 5629'	75
A-7. Core image of Simpson Canyon 1044 interval 5629' to 5658.95'	76

A-8. Core image of Simpson Canyon 1046 interval 5310' to 5355'	77
A-9. Core image of Simpson Canyon 1046 interval 5355' to 5395.2'	78
A-10. Core image of Simpson Canyon 4045 interval 5876' to 5921'	79
A-11. Core image of Simpson Canyon 4045 interval 5921' to 5964'	80
A-12. Core image of Simpson Canyon 4045 interval 5964' to 5996.6'	81
A-13. Core image of Simpson Canyon 5027 interval 5690' to 5710'	82
A-14. Core image of Simpson Canyon 5027 interval 5710' to 5730'	83
A-15. Core image of Simpson Canyon 5027 interval 5730' to 5750'	84
A-16. Correlation of wells with available core illustrating relationships between well logs general lithology	85

INTRODUCTION

In the southern Midland Basin, on the southeast flank of the Central Basin Platform, Early Permian Wolfcampian allochthonous carbonate gravity flows are encountered in the subsurface of Northwestern Crockett County, Texas (Figure 1). These gravity flow sediments hold crucial information pertaining to their origin, their transport processes, and the relationship between both carbonate platform morphology and the response of the platform to base level fluctuations. Understanding these deposits can also help to elucidate the link between processes on the platform shelf and those in the deep basin. These interrelationships can have practical uses in exploration as they can be used to predict the spatial and temporal variations of carbonate materials as well as predicting the location of material prone to porosity development.

Through the use of whole core calibrated to well logs and extrapolated to areas in which core is not available, interpretations were made as to the nature of the deposits. Although the sediments found in the core exhibit extreme heterogeneity, similarities are found in the definition of lithofacies, depositional facies, and log facies. Ultimately, the end result is the recognition of a system of deposits where each is intimately tied into the stage of the environment in which it was produced.

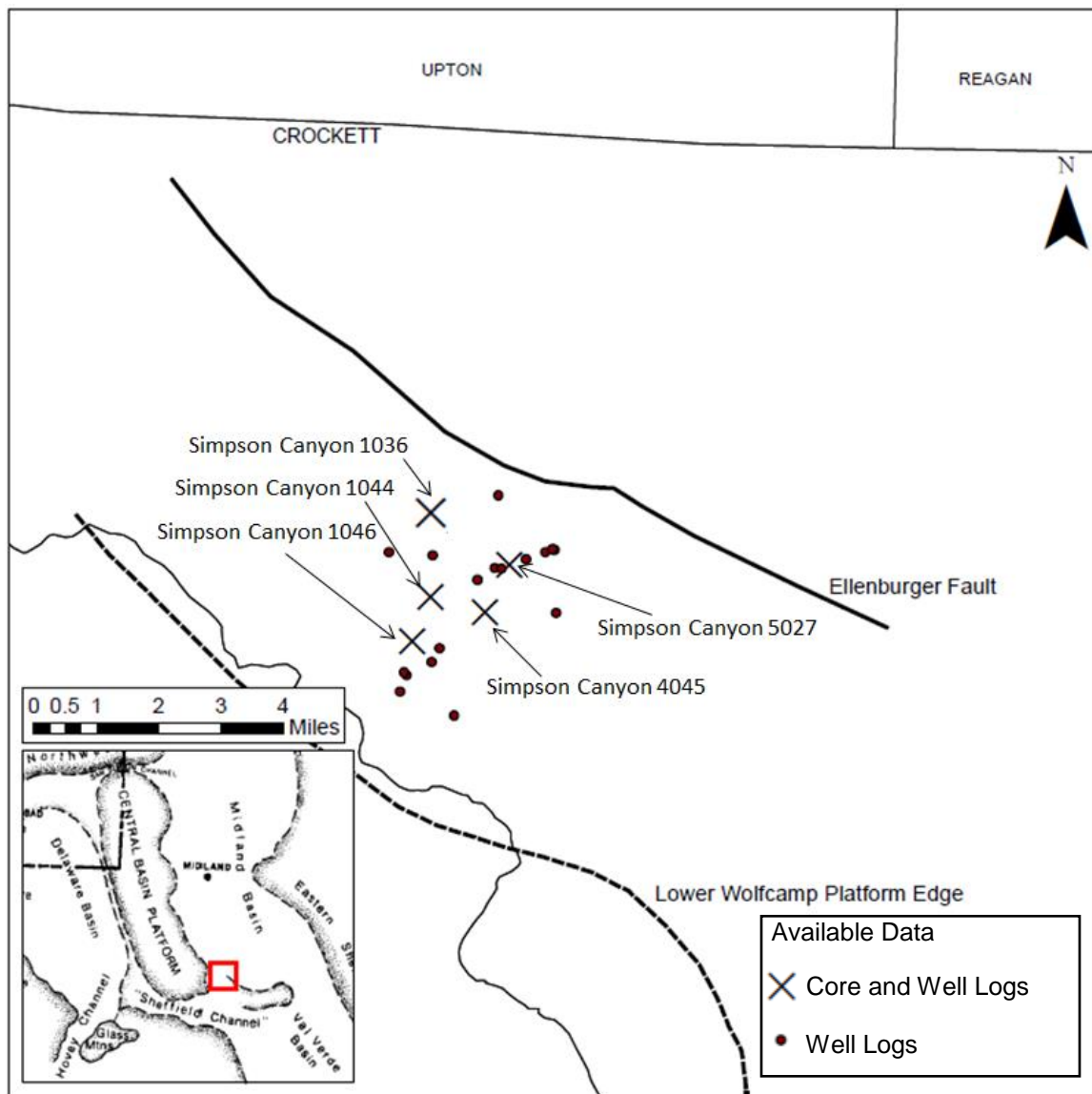


Figure 1. Location of Study area and wells used in study with mapped location of the Lower Wolfcamp platform margin mapped by Hobson, et al. (1985).

STUDY AREA

The location of the cored intervals is in the northwest corner of Crockett County, Texas, approximately 3 miles north of the town of Iraan, Texas, in an area known as Simpson Canyon. The study area (Figure 1) covers approximately 13 square miles and contains 23 wells used in the study, with 5 of the wells containing core samples. The wells were drilled as wildcat wells to exploit the potential hydrocarbons found in Wolfcamp "Reef" strata, similar to those found on the opposite side of the platform in Hockit North, Hockit Northwest, and Nuz fields in adjacent Pecos County, Texas. The location of the wells is on the southeast corner of the subsurface structural feature known as the Central Basin Platform. The wells are located on the northern slope of this ancient carbonate platform, proximal to the paleo-platform margin as mapped by Hobson et al. (1985). The age of the interval of interest is early Permian and the rocks belong to the Wolfcampian Series that extends from 290-280 million years ago.

GEOLOGIC HISTORY

The study area is located in the West Texas Basin where extensive oil and gas exploration has illuminated the geology of the area. When examining the stratigraphic history of the West Texas Basin, three major stages of sedimentation are recognized (Adams, 1965, Ward et al., 1986, and Sarg et al., 1999). The first stage is Lower Paleozoic and ranges from Upper Cambrian to Mississippian when the structural setting was considered passive-margin after the rifting of the Precambrian supercontinent Rodinia. Shallow water sedimentation dominated in this phase with widespread carbonates developed on the great American carbonate bank (Figure 2).

The next phase of sedimentation in the West Texas Basin takes place from the Upper-Mississippian to the Lower Permian during the Ouachita-Marathon Orogeny. During this time, ancestral North America and South America were colliding, creating a crustal flexure in the foreland of the orogenic front. In this foreland basin, widespread deposition of siliciclastics occurred in the early Pennsylvanian followed by carbonate development on the shelves and margins. A major structural feature that developed during this period was the Central Basin Platform, a mafic cored basement high (Adams and Keller, 1996). This crustal block was uplifted so that the single Tobosa Basin was split into several

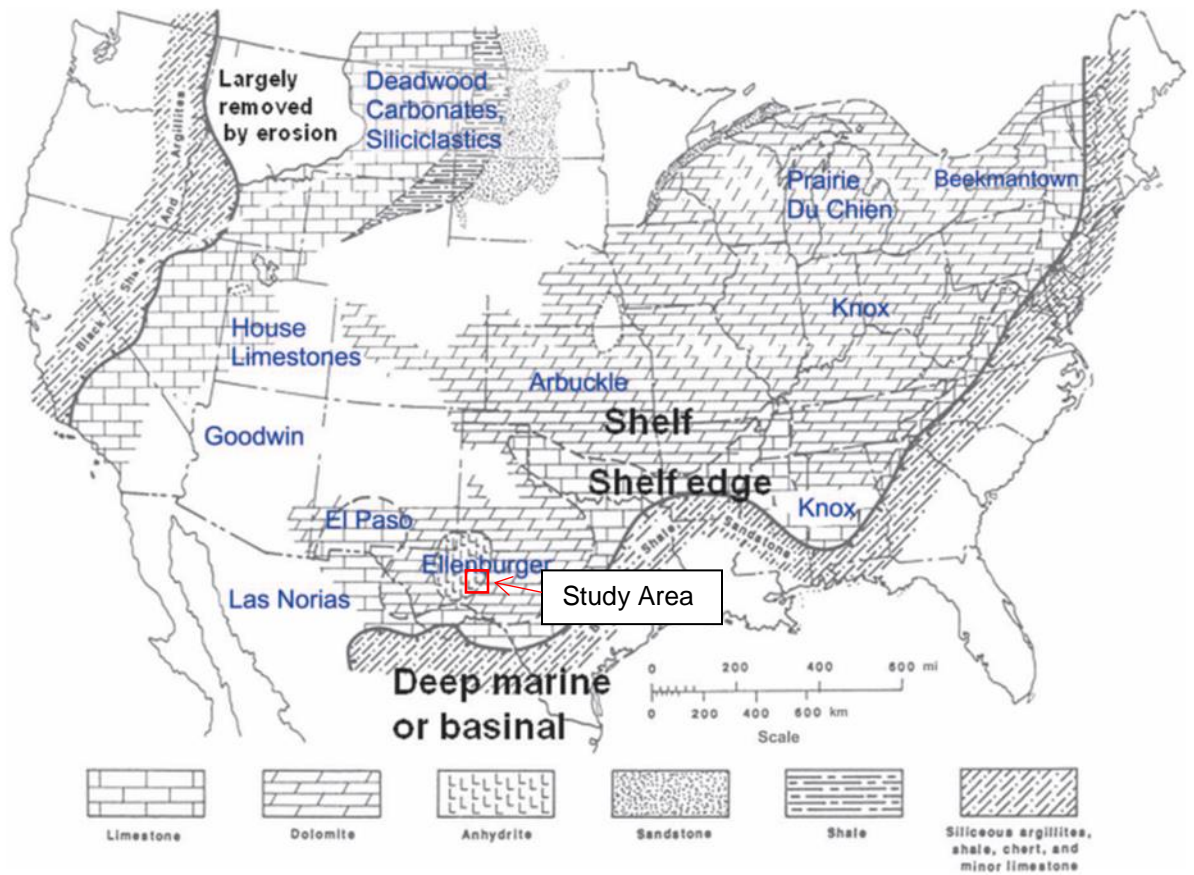


Figure 2. Extent of Ordovician carbonate deposition along the great American carbonate bank (from Sternbach, 2012).

sub basins. These Permian sub-basins include the Midland, Delaware, and Val Verde basins in the configuration seen in Figure 3. Uplift along the Central Basin Platform with subsidence in the flanking basins created abundant accommodation space for sedimentation (Yang and Dorobek, 2012). During this time, carbonate sedimentation was taking place on the shelf and newly uplifted platform areas located in the photic zone. Meanwhile, organic-rich shales and mudstones were being deposited in the deeper, basinal areas. In the Permian Basin, the only outlet to the ocean was the Hovey Channel to the west, which aided in restricting the basins and preserving the organic material. Sequence stratigraphic studies (Sarg et al., 1999) with investigations of global sea level during the Late Paleozoic (Haq et al., 2008) indicates a first order sea level fall as the Absaroka sequence waned. Also, at least three second order sequences in the Permian are recognized along with multiple higher order sequences that affected sedimentation in the Permian Basin (Figure 4). The last phase of deposition in the area is considered the post-orogenic basin-fill from the upper Permian to today. This period is marked by the filling of the Midland and Delaware basins with siliciclastics and a general shift in sedimentation from carbonates into sandstones and evaporites (Ward et al., 1986). Shortly after the fluvial to lacustrine Dockum Formation was deposited, a major unconformity occurs where the region was subaerially exposed before Cretaceous limestones were deposited that cap the area.

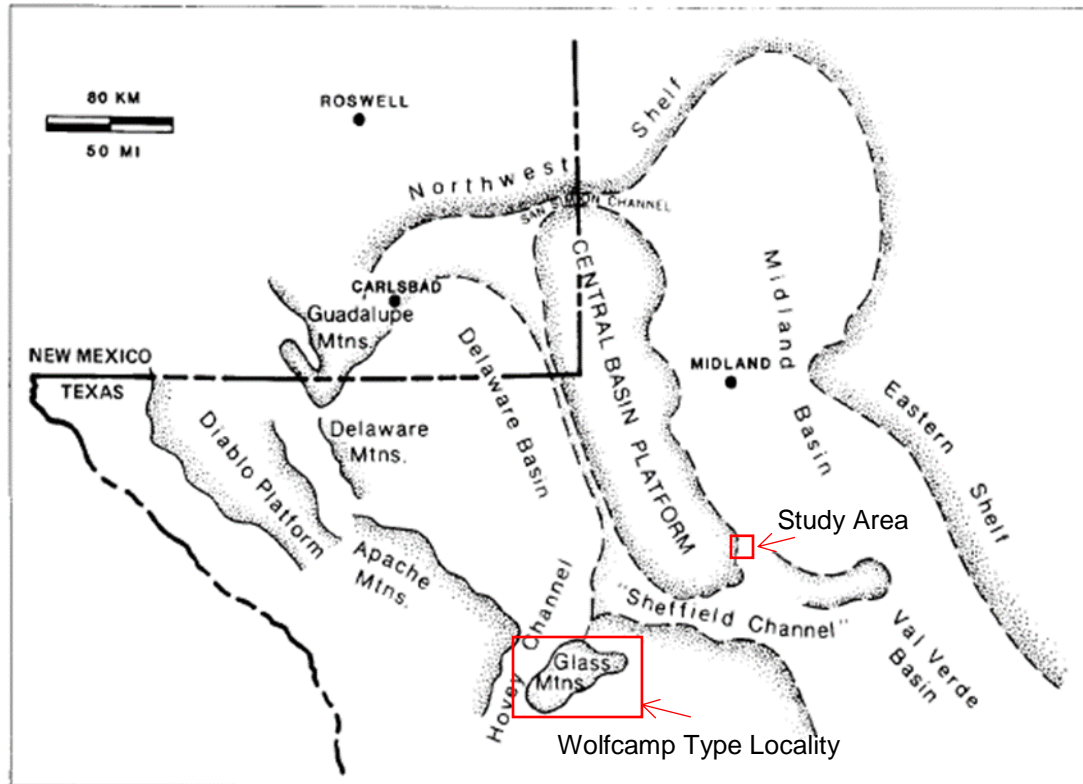


Figure 3. Sub-basin configuration during the Permian with the Central Basin Platform structural high separating the Midland and Delaware basins (from Ward et al., 1986).

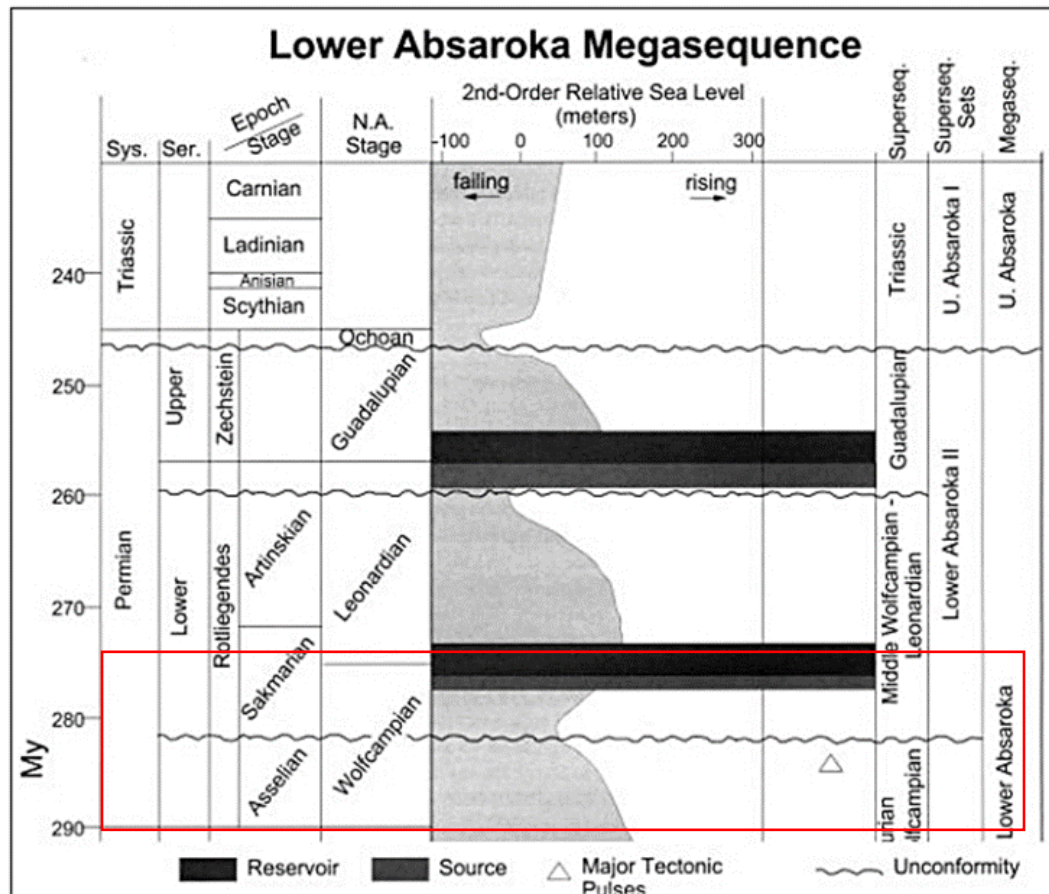


Figure 4. Stratigraphy and 2nd order relative sea level changes for the Permian Basin during the Lower Absaroka megasequence with interval of interest highlighted (from Sarg et al., 1999).

LITERATURE REVIEW

According to the Sellards et al. Bureau of Economic Geology report from 1932, the Wolfcamp Formation, named after Wolf Camp at the type locality, was first defined by Udden et al. (1916) based on outcrops in the Glass Mountains. The type locality of the formation is located 12 miles north of Marathon, Texas, where 700 feet of sediments are exposed. At the type locality, the outcrop consists of shales and limestones with some sandstone and conglomerates. The base of the formation there consists of 100 feet of shale, above which rests a grey limestone member 50 feet thick, followed by thin-bedded limestones and shales approximately 550 feet thick. In 1917, Udden made a more comprehensive study of the outcropping Permian sediments in the Glass Mountains and subdivided them into the following formations: the Wolfcamp, Hess, Leonard, Word, Captain, and Bissett. A later description of the Wolfcamp type locality by Ross (1963) further divides the Wolfcampian in the Glass Mountains into the Neal Ranch and the overlying Lennox Hills Formation, nomenclature that is not in use in the Delaware Basin, Midland Basin, or the Central Basin Platform where the Wolfcampian is divided into Upper, Middle, and Lower Wolfcamp by Candelaria et al. (1992).

The first commercial well in the Permian Basin was completed in the early 1920's. The Santa Rita No. 1 was drilled in Mitchel County to a depth of 2,498

feet and produced for decades until capped in 1990. This discovery led to additional drilling in Crockett County and Pecos County where the World, McCamey, and Yates Field were founded. Exploration efforts grew considerably since, with the Permian Basin expanding to cover an area of nearly 250 miles wide and 300 miles long in West Texas and Southeastern New Mexico, with cumulative production exceeding 29 billion barrels of oil and approximately 75 trillion cubic feet of natural gas as of 2014 (Ewing et al., 2014).

Because of the economic importance of the West Texas Permian Basin, a massive amount of information has been accumulated through exploration efforts. One of the most important papers to come out of this work is P. B. King's 1942 comprehensive examination of the Permian Basin: "Permian of West Texas and Southeastern New Mexico." King's paper covers the entirety of the Permian Basin region from the Pennsylvanian to the present and is arguably the most important piece of literature on the area when looking for an overview. Further work on the area is primarily driven by exploration in the Permian Basin and is based off of well data that is not always available due to its proprietary nature. An example of this includes J. E. Adams' 1965 paper "Stratigraphic-Tectonic Development of Delaware Basin" where the author discusses large scale structural-stratigraphic features based on proprietary well correlations and divides depositional stages into the pre-Pennsylvanian Tobosa Basin and the early and late Permian depositional stages.

Later studies that are more focused on similar areas include Hobson et al. (1985) that looks closely at the carbonate gravity flows and their fauna to the north and east of the study area in Reagan and Crockett counties, along with Loucks et al. (1985) that examined similar gravity flows on similarly aged carbonate slopes in the northwest shelf of the Delaware Basin. Interpretation of these deposits are aided by investigations of analogue carbonate gravity flows in the Bahamas, Indonesia, and elsewhere (Cook, 1983; Middleton et al., 1976; Tanos et al., 2013; and Mullins & Van Buren, 1979). Lastly, with the advent of advanced geophysical surveys and computational simulations, the basement structures and rates of subsidence have been examined by Adams and Keller (1996) and Ewing (2013). While Adams and Keller (1996) utilized magnetic, gravity, and seismic data to determine the configuration and composition of basement structures along the Central Basin Platform and Ozona Arch, Ewing (2013) used computer simulations of deposition integrated with large scale structural information to construct a history of subsidence throughout the different parts of the Permian Basin.

Carbonate Slope Depositional Controls

Carbonate platform depositional environments are known to have numerous controls, both intrinsic and extrinsic, on the type and amount of

sediment produced on the platform and subsequently what is shed into the slope and basin. In this study, platform and slope architecture along with biologic and environmental factors have helped to shape the type of deposits found in the Simpson Canyon area. In fact, these three factors are linked, in that environment and biology exert a control on the architecture of the slope according to Adams and Kenter (2013) and Wahlman and Tasker (2013). The former is a study in which a comparison of siliciclastic and carbonate slopes is made. The authors observed seismic transects of platform and slope morphology and categorized them into three categories based on mathematical expressions for each (Figure 5). They divided slopes into linear, exponential, or gaussian based on the fit of the slope profiles to various styles. Linear slopes were classified as prograding ramps having sediment piled up to the angle of repose; exponential profiles were those that had a sharp increase in declivity at the shelf margin and a concave nature; and gaussian profiles were those with a rounded shelf margin.

When observing the profiles in the Permian Basin, exponential and gaussian styles dominate and transition from the former to the latter through time. Gaussian style profiles are inferred to develop when cycles of base level change erode and round off the shelfbreak. Where exponential profiles dominate, binding organisms are often found to stabilize the shelfbreak, preventing rounding and creating a steep angle with a concave profile beneath. Kerans et al. (2013) observed slope profiles and their evolution through time from the

Wolfcamp to the Guadalupian on the Northwest Shelf of the Permian Basin, and they have developed a model of how this transition took place. The authors suggested that continental glaciation on the Gondwana subcontinent during the Late Pennsylvanian to Early Permian resulted in high-frequency cycles of glacioeustatic sea-level fluctuations. These base level fluctuations are surmised to be the cause of the gaussian slope profile during the time that the study area sediments were deposited. Gaussian slope profiles have minor declivities and no sharp shelfbreak. As continental glaciation ceased around the Leonardian, a shift into greenhouse climates raised sea level and the high-frequency fluctuations no longer rounded off the shelfbreak, resulting in an evolution into exponential slope profiles.

Biologic controls on slope profile and sedimentation were the type of carbonate buildups that are indicative of the late Paleozoic. Wahlman and Tasker (2013) studied the biota of Lower Permian shelf margins and summarized the organisms that occupy, and the morphology of, these “reef mounds.” The reef mounds are carbonate buildups that lack organisms like coral or stromatoporoids, and are instead built by delicate organisms that built structures in the sub-wavebase upper slope setting. These mounds consist of organisms such as Tubiphytes, phylloidal algae, encrusting foraminifera, bryozoans, and calcisponges. These positive relief structures act to shelter landward packstone to grainstone shoals.

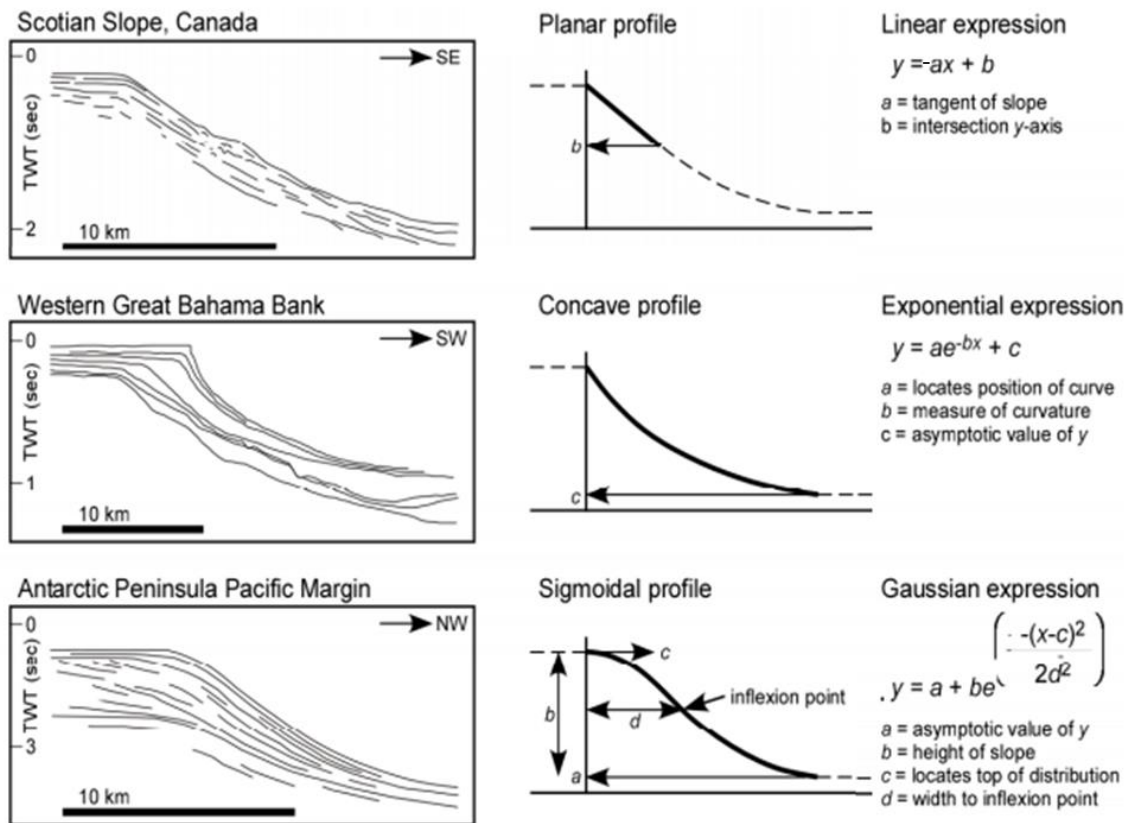


Figure 5. Carbonate slope profiles and their mathematical expressions from Adams and Kenter (2013).

PURPOSE

The objective of this study is to characterize the nature of the rocks found in the Simpson Canyon cores to determine the timing and number of gravity flow events and their relationship to Lower Permian platform carbonates and basinal shales. Studies performed on Lower Permian deposits in the West Texas Permian Basin were primarily concerned with the major production zones either on the Central Basin Platform or in the flanking Midland and Delaware basins. Comparatively, little published work has been completed on carbonate gravity flows despite their importance as potential hydrocarbon reservoirs (Hobson et al., 1985, Cook, 1983, and Loucks et al., 1985). Along with their reservoir potential, cycles of gravity flow deposits and interbedded pelagic sedimentation are potentially related to relative sea-level rise and fall in a way that could help to further link sequences on the platform to those in the basin. The timing of these sequences could illuminate periods of organic matter preservation in coeval basinal Wolfcamp shales and/or platform carbonate drowning or exposure. These transitional sediments between the two zones can act as the link between the two systems where further understanding will expand the knowledge of their interrelationship.

METHODOLOGY

In order to fulfill the objectives of this study, multiple methods of analysis were used, and the results were interpreted in a comprehensive manner. The primary data available for this study are the core and well logs. In the study, five cores with a cumulative 480 feet of 3 ¾ inch diameter slabbed well core was utilized for macroscopic examination of lithology, structures, and relationships. Cores are described in detail and high-resolution photographs taken for all samples both at large and small scales where required.

Along with core, 15 thin-sections were obtained and described petrographically for lithology, nature of allochems, and diagenetic features. Billets were cut from representative lithofacies and sent to Tulsa Sections, Inc. in Coweta, Oklahoma where thin-sections were processed. These thin-sections were studied under the petrographic microscopes at Stephen F. Austin State University where petrographic descriptions, photomicrographs, and high resolution scans were made.

Lastly, the lithologic data was plotted alongside the corresponding well logs where calibrations linked the two. This aided in correlation across both the study area, and into the platform and basin environments. The abundance and availability of well logs from the Bureau of Economic Geology is much

appreciated and was helpful in determining the spatial extent of gravity flows and how these correlate with platform and basinal Wolfcamp deposits.

STRATIGRAPHY

Stratigraphic relationships (figure 6) of Wolfcampian sediments encountered in the Simpson Canyon cores are difficult to correlate to the Wolfcamp type locality due to variability in geologic setting and variable nomenclature. At the type locality in the Glass Mountains of West Texas, the outcrop consists of shales and limestones with some sandstone and conglomerates. The base of the formation is of 100 feet of shale, above which rests a grey limestone member 50 feet thick, followed by thin-bedded limestones and shales approximately 550 feet thick (Udden et al., 1916). This description depends on where the Wolfcamp is located, whether in the type locality, on the Central Basin Platform, or in the Delaware or Midland sub-basins.

Nomenclature has varied through time as subdivisions of the Wolfcampian stage in the Permian Basin were recognized and divisions into the Heuco, Neal Ranch, Hess, and Lennox Hills Formations were made (Adams et al., 1939; Ross, 1959; Flamm, 2008). These formation divisions were useful in outcrop but short-lived due to their inability to correlate with subsurface deposits. Both

AGE		STRATIGRAPHIC UNIT			
SYSTEM	SERIES	DELAWARE BASIN	CENTRAL BASIN PLATFORM	MIDLAND BASIN	EASTERN SHELF
PERMIAN	Ochoan	Dewey Lake	Dewey Lake	Dewey Lake	
		Rustler	Rustler	Rustler	Rustler
		Salado	Salado	Salado	Salado
		Castile	Castile		
	Guadalupian	Bell Canyon	Capitan Reef	Tansill	Tansill
				Yates	Yates
				Seven Rivers	Seven Rivers
				Queen	Queen
				Grayburg	Grayburg
		Cherry Canyon	San Andres	San Andres	San Andres
		Brushy Canyon			
	Leonardian	Bone Spring	Clear Fork	Spraberry Dean	Clear Fork
			Tubb		
	Wolfcampian	Wolfcamp	Wichita	Leonard	Wichita
			Wolfcamp	Wolfcamp	Wolfcamp
PENNSYLVANIAN	Cisco Canyon	Cisco	Cisco	Cisco	Cisco
		Canyon	Canyon	Canyon	Canyon
	Strawn	Strawn	Strawn	Strawn	Strawn
	Atokan	Atoka	Atoka	Atoka	Atoka
					Bend

Figure 6. Generalized stratigraphic column throughout the Permian Basin with approximate study area interval highlighted. (Modified from Mazullo and Reid, 1989)

Industry and the North American Stratigraphic Code have chosen to simplify matters by utilizing the terms “Wolfcamp” or “Wolfcampian” for formation and stage names (Flamm, 2008) which will be used in this study. Basinal Wolfcamp is described as thick packages of black siliceous shales interbedded with calcareous shale and limestone with a maximum thickness of approximately 1700 feet in the deepest portions of the basin and a general trend of deepening to the south (Hamilin and Baumgardner, 2012). Late Pennsylvanian to Wolfcampian deposits on the Central Basin Platform consist of approximately 1600 feet of strata that thin onto structural highs to the west (Saller et al., 1994). On the eastern Central Basin Platform, Wolfcamp sediments studied by Saller et al. (1994) consist of green and red shales and sandstones and overlying carbonates consisting of grainstones, wackstones and packstones, and algal boundstones. Features in these sediments include evidence of cyclic subaerial exposure in the form of vugs, fissures, root traces (rhizoliths), and caliche crusts. Proximal to the Central Basin Platform and Eastern Shelf of the Midland Basin, the Wolfcamp is composed of allochthonous shallow water carbonate gravity flows underlying both siliceous and calcareous shales (Hobson et al., 1985; Loucks et al., 1985; Mazzullo and Reid, 1987; Mazzullo, 1997).

Divisions of the Wolfcamp on the periphery of the basin, such as those in the study area of interest, are difficult to correlate to basinal and platform Wolfcamp and include operational nomenclature based on log characteristics

such as the Wolfcamp “Reef” used to describe blocky carbonate log signatures similar to how the actual reef material presents on the platform, and low gamma ray Wolfcamp Shale for hemipelagic deposits of fine grained material that represents both suspension settled sediments and turbidite deposits. In reference to the age of the Wolfcamp Formation, at the Glass Mountains type locality and in much of the Permian Basin, the Wolfcamp had been accepted as the lowermost Permian formation (Adams et al, 1939). Later, further studies of micro-fossils extended the base of the Wolfcamp formation into the upper Pennsylvanian and the Wolfcampian Leonardian boundary into the lower Leonard Formation with ages constrained by conodont and fusulinid biostratigraphy (Ritter, 1995; Chernykh and Ritter, 1997; Flamm, 2008).

LITHOFACIES

Strata encountered in the Simpson Canyon study area well cores are divided into five lithofacies and are listed based on decreasing volumetric abundance in cores:

1. Bioclast packstone to grainstone facies
2. Porous, bioclast packstone to grainstone facies
3. Lithoclast rudstone and floatstone facies

4. Massive to laminated shale facies
5. Bioclast and lithoclast wackestone facies

Terms used in the classification of the carbonate rocks encountered are derived from Dunham (1962), and the modifications of Dunham's classification to include rudstone and floatstone for coarse grained carbonate gravel employed by Embry and Klovan (1971). This modification retains the classification of allochthonous material as either mudstone, wackestone, packstone, or grainstone, but consideration is also made for the size of allochems instead of simply the grain to matrix relationships. The addition of floatstone and rudstone is to distinguish between large and small allochems where these classes are defined as consisting of 10 percent or more allochems larger than 1/16th of an inch, also described as carbonate conglomerates. Floatstone and rudstone are distinguished from each other by the grain to matrix relationships where rudstones are grain supported and floatstones are "floating" in a finer grained matrix. This division of larger grain size is conducive to understanding the energy required to transport these larger particles.

Bioclast packstone to grainstone lithofacies

The bioclast packstone to grainstone facies consists of relatively homogeneous and massive to fining upward deposits of rounded to subrounded, well to moderately well-sorted bioclasts with examples in figures 7 and 8. The skeletal material is predominately micritized and is contained within a sparry calcite cement in grainstones. In packstones, grains are often slightly more angular and the dark muddy matrix is sparse as grains are tightly packed. Where allochems are elongate, they exhibit a slight imbrication and have a preferred orientation compared to equant grains. When skeletal material is preserved and internal structures are not micritized, it appears that allochems are abundantly crinoid fragments, encrusting and mobile foraminifera, and small brachiopod, bivalve, and bryozoan fragments. A large proportion of allochems have been altered to a state where only a shadow of the former structure may be gleaned, in this case, allochems are often classified as pelloidal due to a spherical nature and micritic composition. Structures and features found in the packstone to grainstone facies include stylolites between contrasting lithofacies, which often occur at high angles, possibly representing scour surfaces where subsequent flows have removed material. Also, periods of quiescence between flows deposit dark laminated mudstone recognized as shale “breaks,” along with zones of intense vertical fractures filled with precipitated calcite.

Simpson Canyon 1036

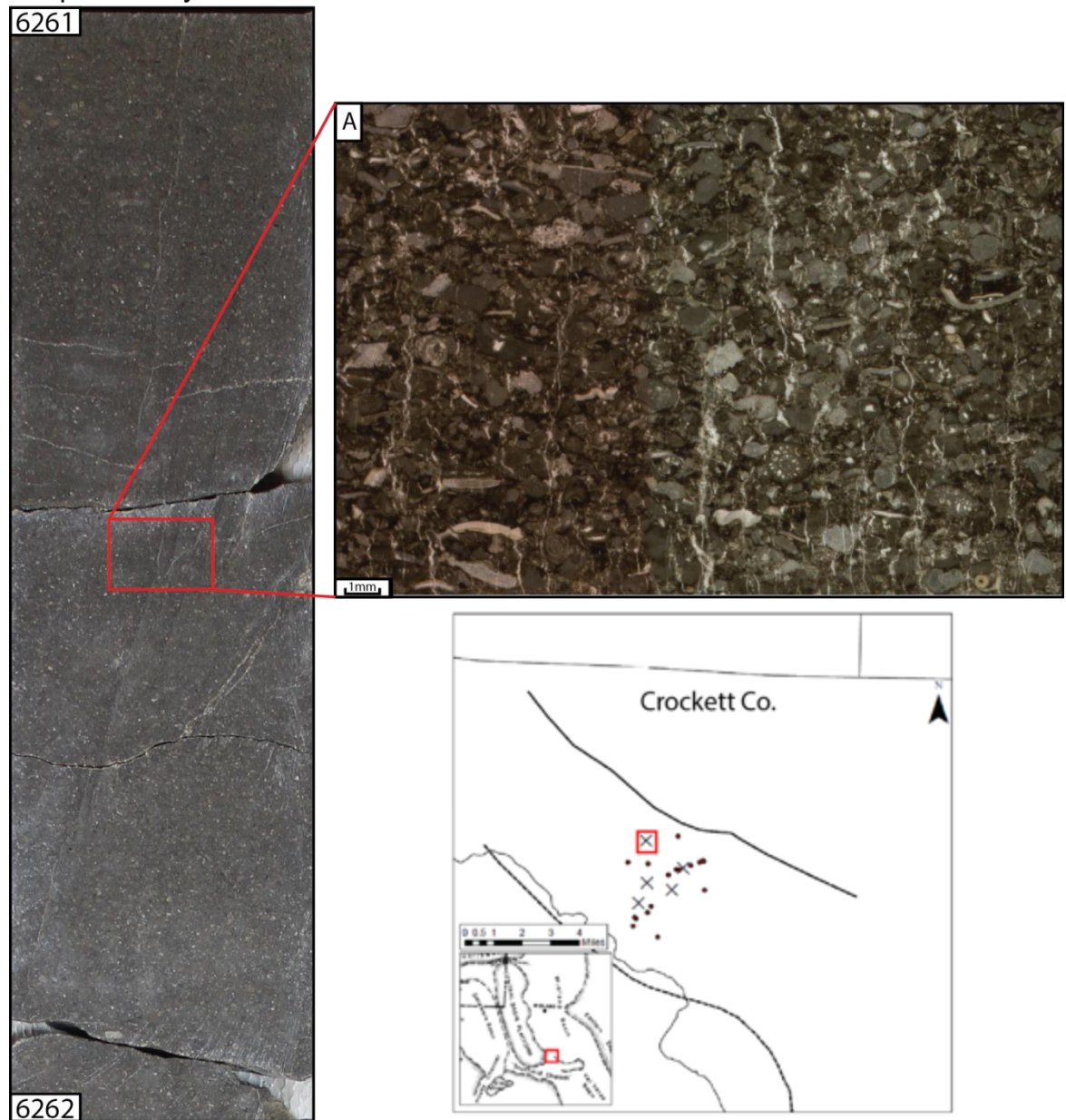


Figure 7. Example of bioclast packstone to grainstone lithofacies in Simpson Canyon 1036 A) Bioclast packstone thin-section of with abundant vertical fractures filled with calcite.

Simpson Canyon 1046

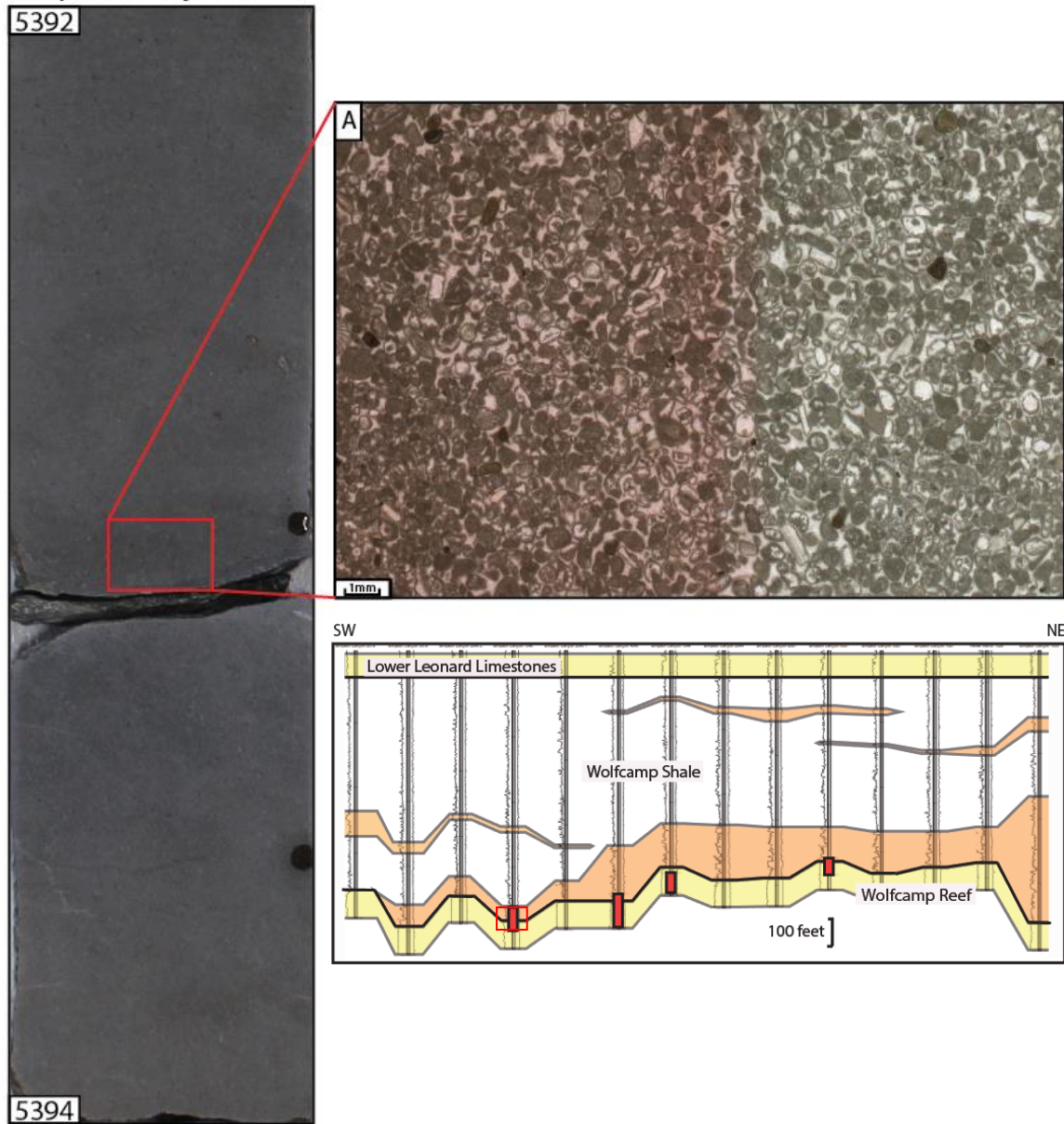


Figure 8. Example of bioclast packstone to grainstone lithofacies in Simpson Canyon 1046 with thin shale break midway through core. A) Thin-section with sand-sized micritized bioclasts of primarily fusulinid foraminifera.

Porous bioclast packstone to grainstone lithofacies

Porous bioclast packstone to grainstone facies (figure 9 and 10) are lithologically similar to the non-porous bioclast packstone to grainstone facies aside from the extensive development of both intra- and interparticle porosity. Porous facies appear to have experienced extensive dissolution of internal structure of allochems while micrite envelopes remain intact. The interparticle porosity is well developed, and both types of porosity show no overall pattern in distribution throughout the cores in the study area. Limited porosity features also found in this facies include vuggy, moldic, and some fracture porosity; however, these are secondary as the inter- and intraparticle porosity structures are vertically continuous in cores, with up to 20 feet of high porosity material. Conservative estimated porosity values from thin-section image analysis software JMicroVision range from 9-13 percent of total volume in the porous facies.

Lithoclast rudstone to floatstone lithofacies

Lithoclast rudstone to floatstone facies (figures 11 and 12) consist of fining upward sequences of resedimented clasts with both rounded lithoclasts to stylolite breccia clasts up to a maximum encountered diameter of 4 inches although larger clasts could extend past the core diameter.

Simpson Canyon 1046

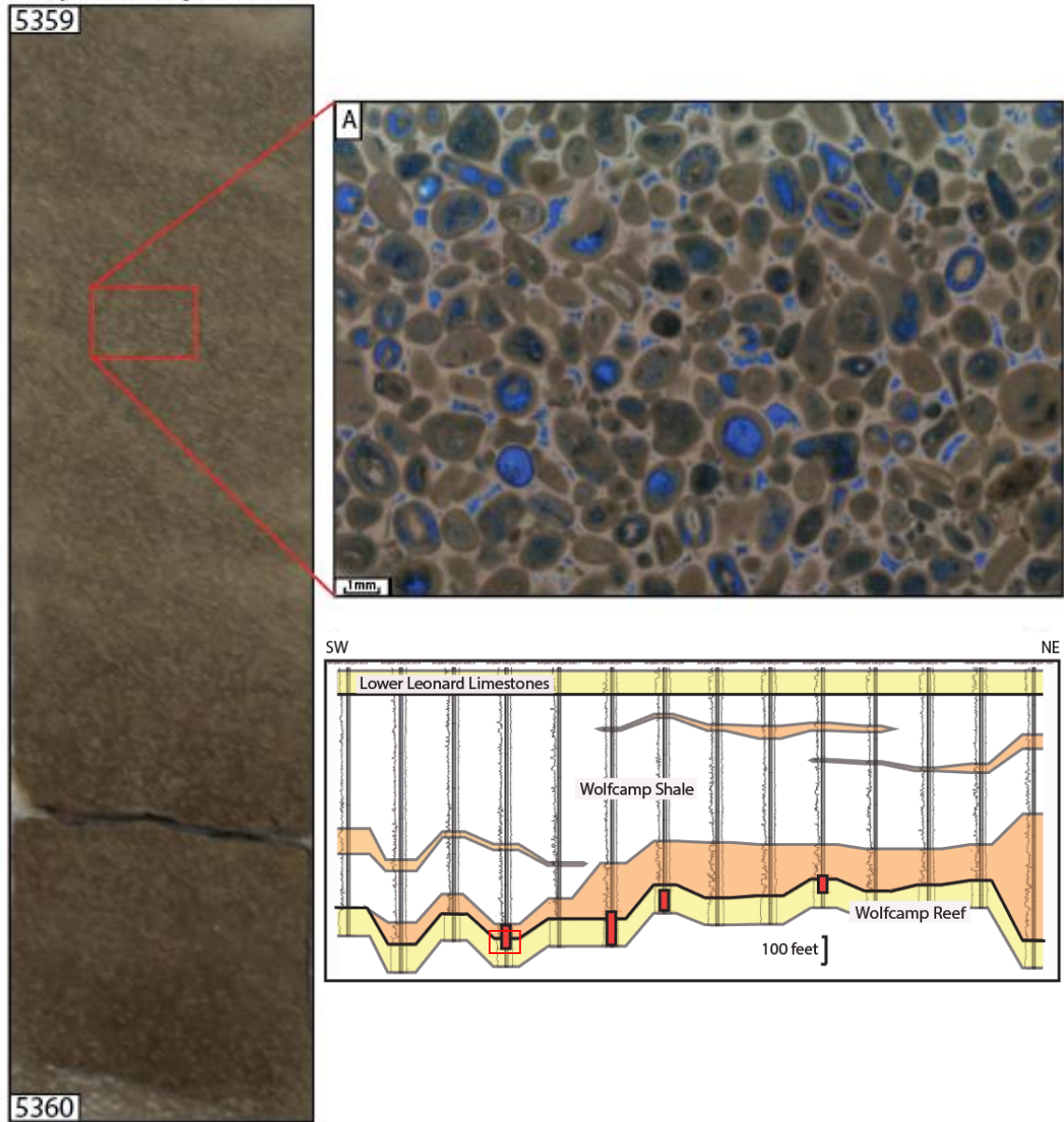


Figure 9. Example of porous bioclast packstone to grainstone lithofacies. Core image of porous bioclast packstone to grainstone lithofacies in Simpson Canyon 1046. A) Thin-section image illustrating the abundant inter- and intra-particle porosity in the pelloidal grainstone

Simpson Canyon 5027

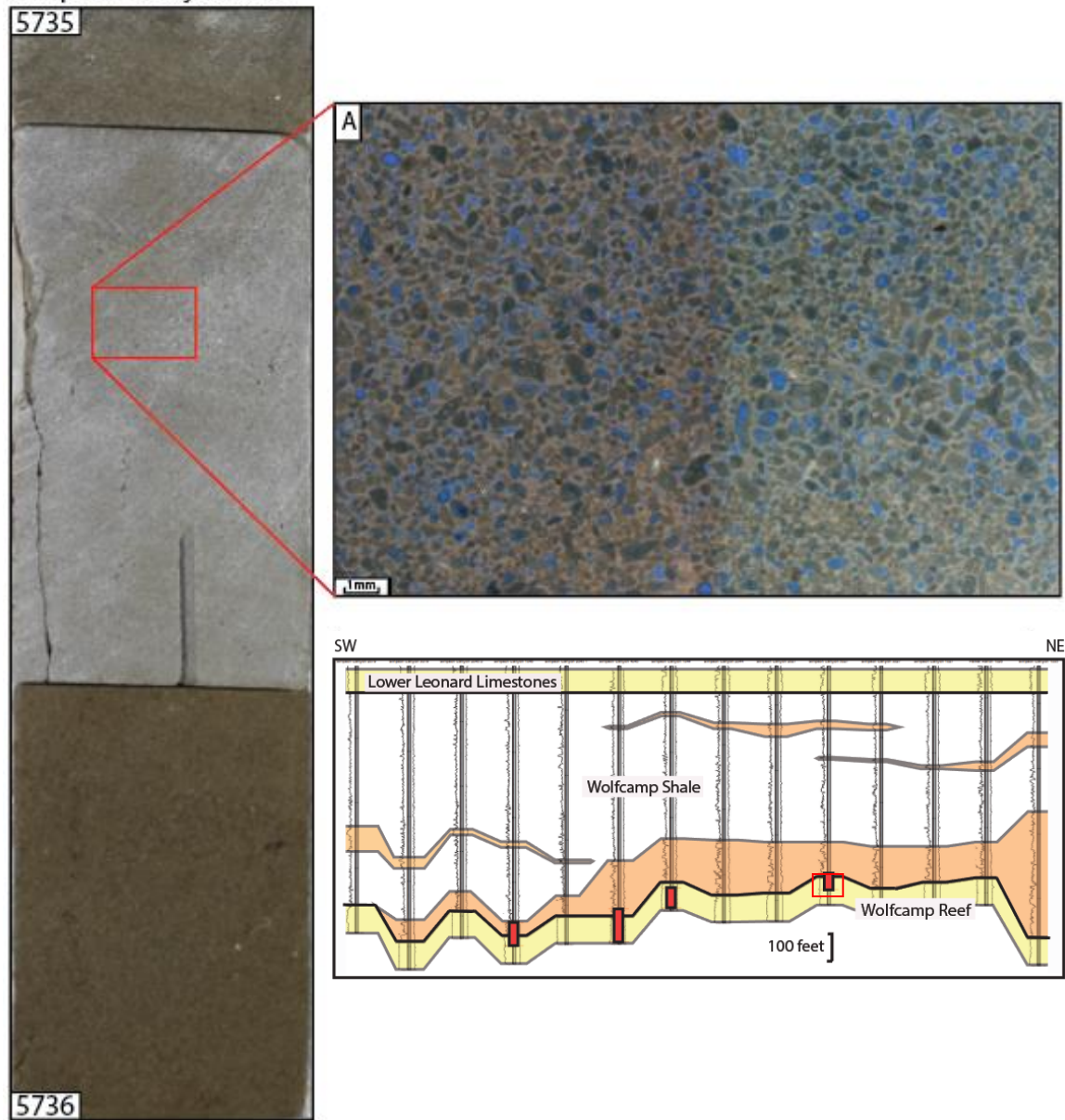


Figure 10. Example of porous bioclast packstone to grainstone lithofacies. Core image of porous bioclast packstone to grainstone lithofacies in Simpson Canyon 5027. A) Thin-section image illustrating similar porosity relationships in a finer-grained lithology.

Simpson Canyon 4045

5983



5984

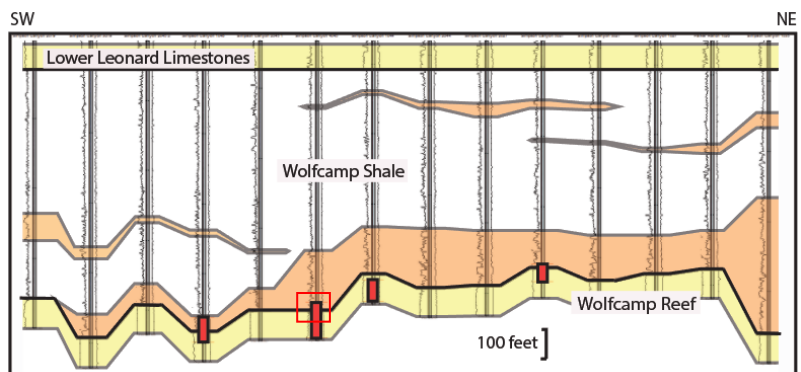
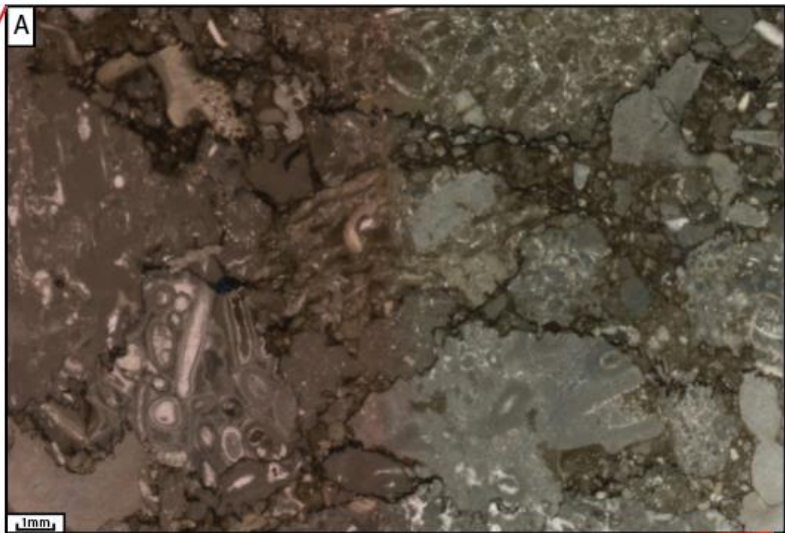


Figure 11. Examples of lithoclast rudstone to floatstone lithofacies. Core image of lithoclast rudstone lithofacies in Simpson Canyon 4045. A) Thin-section image of with lithoclasts of various lithologies and stylolite breccia relationship.

Simpson Canyon 1036

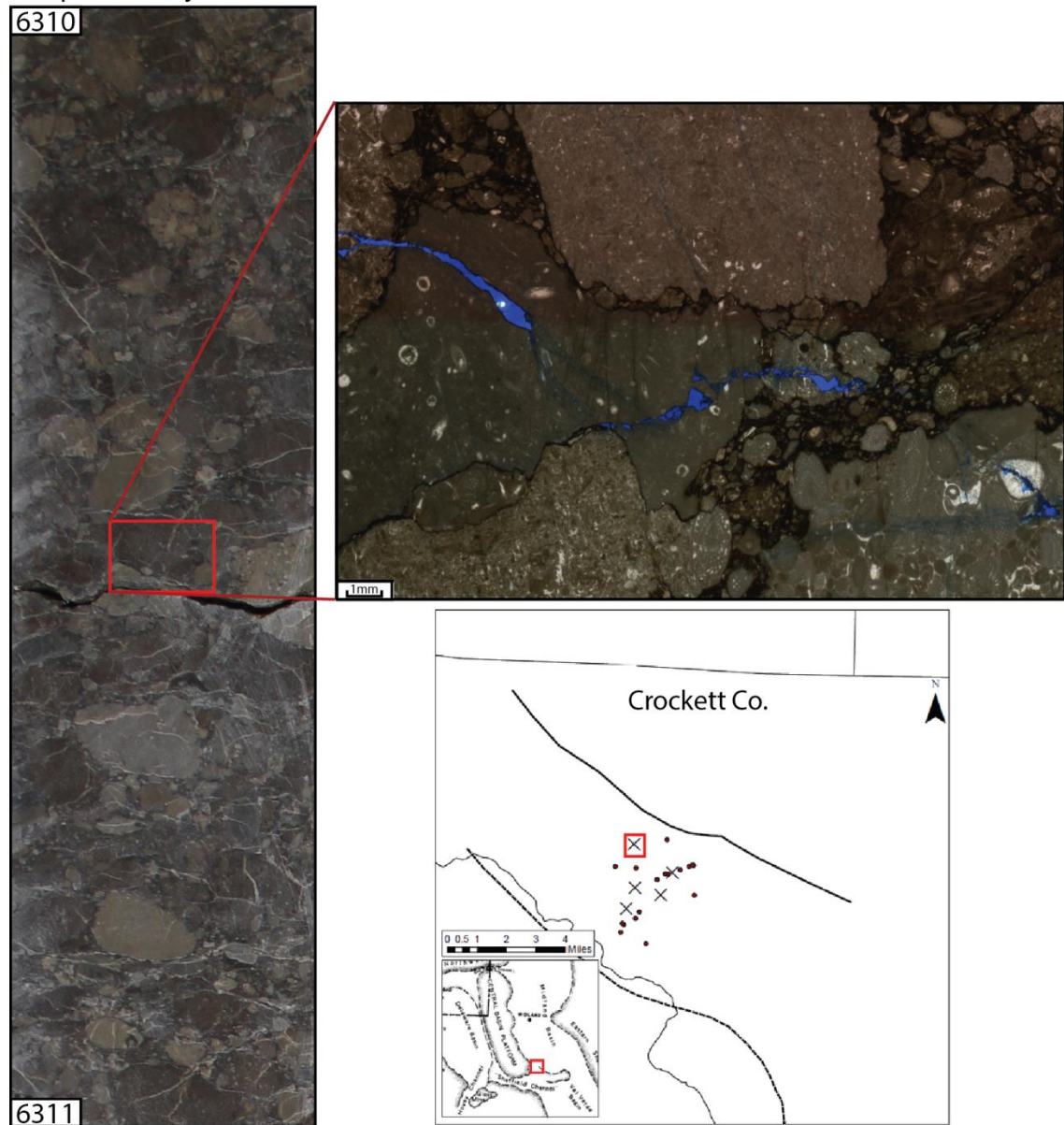


Figure 12. Example of lithoclast rudstone to floatstone lithofacies. Core image of lithoclast rudstone lithofacies in Simpson Canyon 1036. A) Thin-section image of with lithoclasts of various lithologies with bioclast packstone matrix.

Lithoclasts have a diverse lithology including peloidal wackestone, oolitic packstone, mudstone, skeletal grainstone and packstone, and algal boundstone. Matrix material in the lithoclast rudstone facies is predominately loose skeletal packstone with a dark muddy matrix. In the floatstone facies, massive mudstone forms the matrix; however, the larger lithoclasts are likely not syngenetic and represent dropping of material into a muddy interface. Where matrix is lacking, lithoclasts are sutured together with stylolites and a mosaic of stylo-breccias are found. Otherwise, grains are relatively rounded. Allochems encountered in the lithoclasts include peloidal grains of unknown origin, brachiopod, bivalve, crinoid and bryozoan fragments, abundant fusulinid foraminifera, mudstone lithoclasts, tubiphytes, phylloidal algae, and green algal plates. No lithoclasts in this facies exhibit porosity despite some bioclast packstone and grainstones resembling closely the previously described porous lithofacies.

Massive to laminated shale lithofacies

The massive to laminated shale facies (figure 13) consists of dark black to dark grey carbonate mudstone and thinly laminated carbonate-rich shale. In this facies, abundant, sub-horizontally inclined black organic laminae appear along with sparse skeletal material. The shale facies is often interbedded with the wackestone or bioclast grainstone to packstone facies. It also makes up the

Simpson Canyon 5027

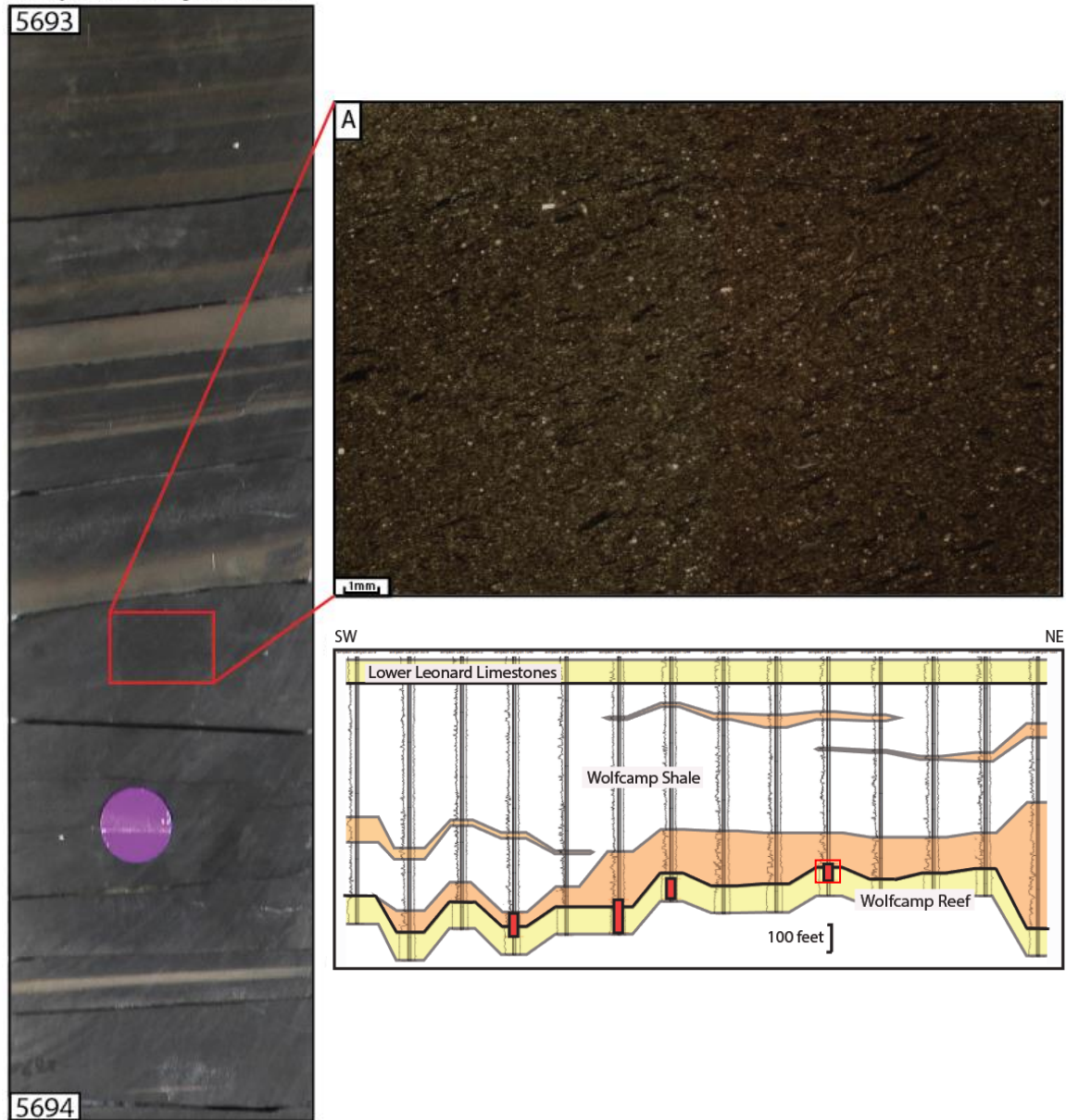


Figure 13. Example of laminated to massive shale lithofacies in Simpson Canyon well 5027. A) Thin-section image showing abundant thin strings of black organic material and sub-horizontal orientation

topmost unit in fining upward sequences. In the laminated shales, thin, light colored laminae occur with regularity and lie inclined at slight to higher angles with occasional convoluted bedding and soft sediment deformation structures. Also, intersected in the core are apparent ripple marks in contact with overlying massive mudstone along with both normal and reverse micro-faulting and deformed laminations due to a dropped lithoclast. Aside from forming thick, continuous beds of shale and interbedded shale and packstone and grainstone, the shale facies also appears as laminated and massive shale “breaks” between gravity flows during periods of quiescence.

Bioclast and lithoclast wackestone lithofacies

The least abundant lithofacies in the cored intervals contains bioclast and lithoclast wackestones (figure 14) with a dark muddy matrix. This lithofacies is often interbedded with the shale and bioclast packstone to grainstone facies where it occurs. Contacts with underlying units are sharp, inclined erosional features and often fine upward into fine grained laminated shale facies. Sorting in this lithofacies is generally moderate to poor and preferred orientation is observed in elongate grains that imply flow. Allochems in this unit are lithoclasts composed of similar lithologies to the bioclast packstone to grainstone facies

Simpson Canyon 4045

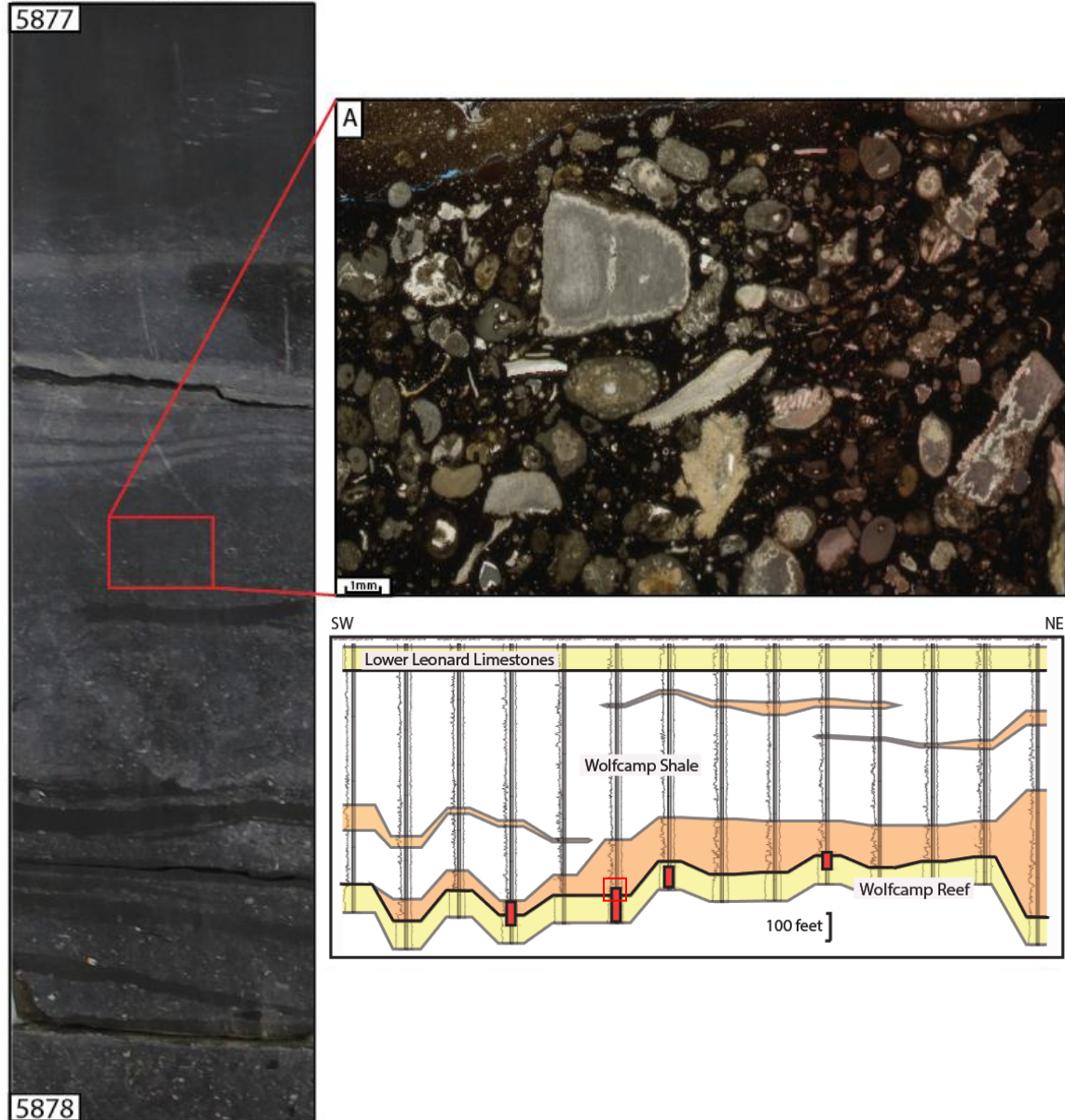


Figure 14. Example of bioclast wackestone to packstone lithofacies in Simpson Canyon well 4045. A) Thin-section image of bioclast wackestone in Simpson Canyon 4045 with abundant broken skeletal debris, fusulinid foraminifera, and crinoid fragments.

along with bioclasts of crinoid, brachiopod, bivalve, and bryozoan, fragments, fusulinid foraminifera, and green algal plates.

LOG FACIES AND CORE CALIBRATION

Calibration of lithologies found in core with their respective wireline log response is difficult, in that the vertical resolution of wireline logs often leads to the inability to discern thin-bedded and interbedded series. This is easily identified in the gamma ray log responses of the interbedded shale and grainstone or rudstone. Although in ideal circumstances, the fine-grained lithologies would exhibit a high gamma ray response due to naturally occurring radioactive materials such as thorium and potassium that preferentially bond to clays or uranium which preferentially bonds to organic matter. The source of the radioactivity in shales can be determined by spectral gamma ray reading; however, the gamma ray logs used in this study do not distinguish between radioactive emitters and thus an average reading is obtained. Aside from radioactive sources being averaged, small interbedded layers are averaged as the vertical resolution of the gamma ray log is approximately 12 inches so that thinner layers of shale and carbonate will be read as halfway between the actual values of both.

This coarse vertical resolution issue extends to the other types of wireline logging tools used in the study so that designations into log facies must take this deficiency into account. Also, only the top of the Wolfcamp “Reef” is encountered in core samples with relatively few samples of the Wolfcamp Shale. Due to this, assumptions have to be made for the character of lithologies encountered outside of sampled wells and depths based on the limited data available. In all, there is a total of 22 wells in the 13 square mile study area with the logs available being primarily gamma ray, photoelectric factor, neutron density, density porosity, and a few resistivity logs. Log facies have been defined based on gamma ray and photoelectric factor due to most wells possessing these logs; however, relevant information pertaining to the other tools will be mentioned when available. An example log calibration with average log values and lithofacies is shown in figure 15. Log facies used for calibration and correlation are:

1. Thick-bedded log facies
2. Porous log facies
3. Thin-bedded log facies
4. Shale log facies

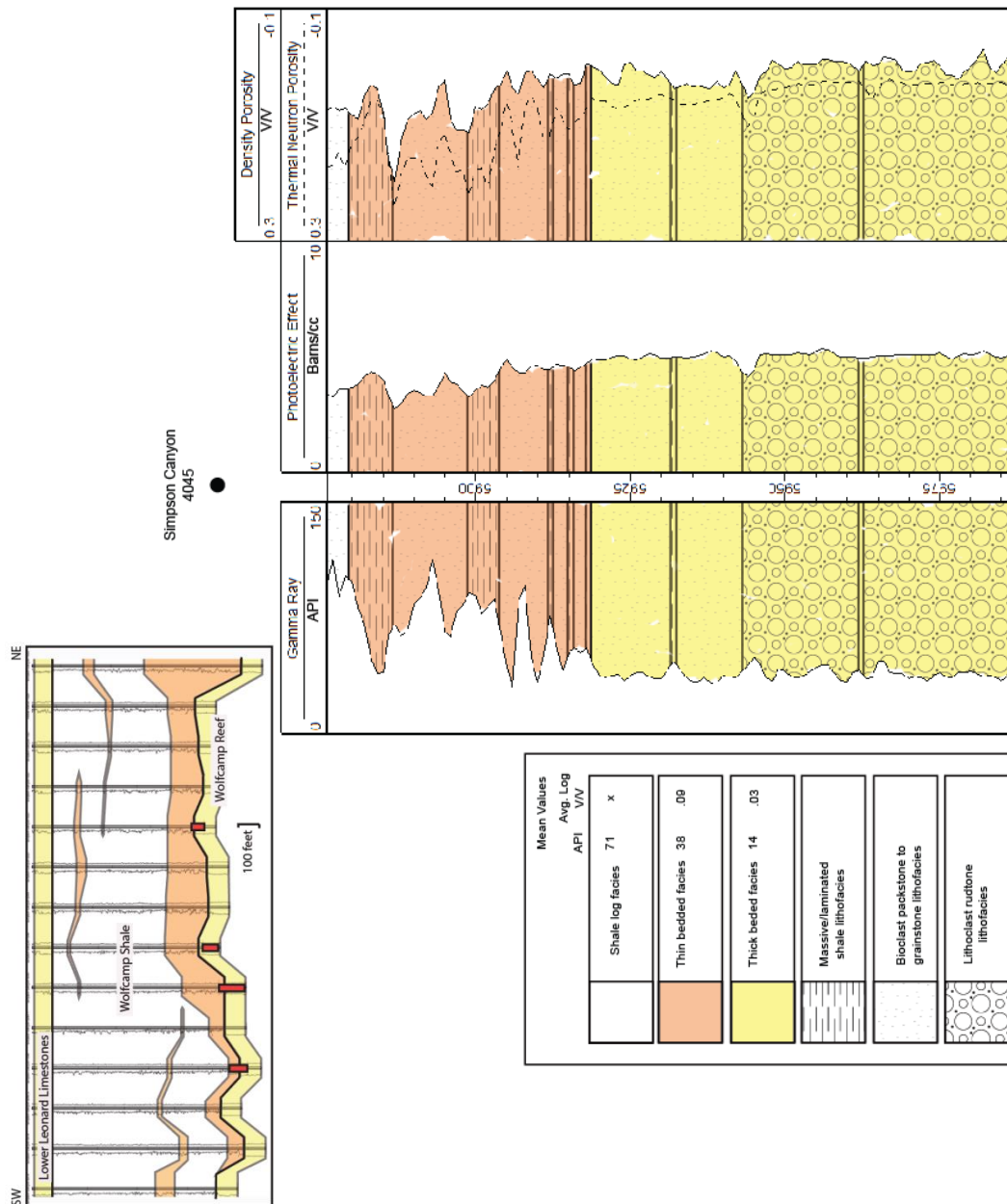


Figure 15. Simpson Canyon 4045 well log calibration with average log readings and lithofacies plotted.

Thick-bedded log facies

The thick-bedded log facies represents the Wolfcamp “Reef” and is characterized by a blocky, low gamma ray log reading that is laterally continuous throughout the study area. This facies is not penetrated through completely in all wells and so the total thickness and variation of thickness throughout the study area is not well constrained. Where available, maximum thickness of the thick-bedded log facies is at least 450 feet and is cut off by the end of the log, but may continue at depth. This log facies is also characterized by a consistent reading of approximately 5 barns per cubic centimeter in the photoelectric factor log which is indicative of relatively pure carbonate rock. Occasional gamma ray spikes correspond with low readings in the photoelectric factor that may indicate the presence of thicker shale interbeds with some siliciclastic influence. These thick shale interbeds are not encountered in the core despite occurrences of very thin shale “breaks” in the core that are under the vertical resolution of the wireline logs and are not discernable in the data. Resistivity and both neutron and density porosity readings in this log facies are generally low and increases markedly in the porous facies that is contained within the thick bedded log facies. Low readings for both of these logs are not surprising as the lack of pore space due to fully occluding calcite spar cement increases the electrical conductivity through

the rock. The lithofacies representing the thick-bedded log facies include both the bioclast packstone to grainstone facies and often overlying lithoclast rudstones.

Porous log facies

The porous log facies lies within the thick-bedded log facies and shares the same very low gamma ray and carbonate photoelectric factor signatures. The distinguishing feature of this facies that sets it apart from the previous log facies is the abundant porosity characterized by the high readings in the neutron and density porosity logs. Average porosity from both porosity logs range from 1-12.4 percent porosity. Resistivity logs also give high responses compared to the surrounding non-porous facies due to the inability of open pores to conduct electricity well. This log facies is calibrated with core data reasonably well, in that thin sections of core samples from the intervals display abundant inter- and intraparticle porosity with estimated values of approximately 9-13 percent porosity based on image analysis software. The lithology of the porous log facies is the same as the previous log facies except for the extensive dissolution of both matrix and grains. Porosity development observed in the logs appears to be chaotic and discontinuous throughout the study area.

Thin-bedded log facies

The thin-bedded log facies overlies the thick-bedded log facies and appears to be a transitional facies between the underlying blocky and massive gamma ray log readings and the generally high gamma ray readings of the shale facies. The gamma ray log response in this zone is chaotic and varies from the lowest of values like those found in clean carbonates to the highest of gamma ray responses such as those in a clean shale. In some wells, this log facies has a fining upward character and even exhibits multiple sequences of fining upward. Photoelectric effect in this log facies is also characteristically variable showing values of around 5 in zones of low gamma and lower values in zones of high gamma. Resistivity logs and neutron and density porosity logs also show variability with low resistivity in the carbonate rich zones, high resistivity in the organic rich shale, and anomalous high porosity log readings in the shale due to bound water known as the “shale effect.” Lithologies encountered in the thin bedded facies vary from laminated mudstone and shale interbedded with either bioclast wackestone to grainstone or lithoclast rudstone to floatstone. When calibrated with core, both lithologies are found interbedded and log response cannot be used to infer whether the lithology of the carbonate is rudstone to floatstone or wackestone to grainstone due to similar readings and limited vertical resolution. The maximum thickness of this log facies is 207 feet and has

two distinct lobes that appear to thicken basinward and are absent proximal to the shelf margin. These are interpreted to represent the debris flow depositional facies where a large plug of debris leads at the front of the flow and creates a barrier to prevent bypassing of subsequent flows so that a backstepping of gravity flows occur until the topography is filled in.

Shale log facies

The shale log facies consists of mostly continuous high gamma, low photoelectric factor readings with very thin interruptions of low gamma and medium photoelectric factor responses typical of carbonates. Other log responses include generally high resistivity, likely due to organic richness of the shale, along with high neutron porosity readings due to bound water in clays. The tool response in this log facies is used as the basis for recognition of the Wolfcamp Shale interval with thick continuous shale deposition of up to 830 feet. Rarely, interruptions of the previous thin-bedded facies occur as possible collapse events; however, these extend less and less into the basin through time and are interpreted to represent periodic failure along a backstepping reef margin. Core calibrations of this log facies are restricted to the interbedded units as the bulk of the continuous Wolfcamp Shale was not cored; although, the very top of the Wolfcamp Shale was cored in a single well and the shale resembles

the units found in the interbedded facies along with having similar log responses. This is not definitive evidence to the claim that the shale facies is continuous considering that it is unlikely that changes have not occurred during 800 feet of deposition.

INITIATION, TRANSPORT, AND RELATIONSHIP OF GRAVITY FLOWS

Mapping of the study area, well log correlations, and observed lithofacies relationships in core suggest that upper Pennsylvanian and lower Permian materials found in the Simpson Canyon area were deposited on the slope of a north north-eastern dipping carbonate ramp. Resedimented platform detritus interbedded with laminated basinal mudstones suggest failure along the platform margin and transport of shelf derived lithologies into lower slope and basinal settings. Initiation of rockfalls, slides, and sediment gravity flows can be caused by tectonism, storm and tsunami action, subaerial erosion during sea level lowstands, and higstands shedding due to over steepening of slopes. These initiation mechanisms result in the downslope movement of large amounts of shelf and upper-slope sediments under gravity into distal settings to be resedimented.

Sediments are transported away from the shelf and upper-slope through four primary gravity flow processes that result in varying products, which include:

(1) Turbidity currents: resulting in partial or complete Bouma sequences, typically fining-upward turbidite sequences which vary in thickness and may extend considerable distances from the origin; (2) Grain flows: resulting in coarsening-upward sequences of limited thickness and distance from origin; (3) Fluidized/Liquefied flows: flows where grains are buoyantly supported by the upward movement of pore fluid, temporarily suspending them. Deposits are typified by the presence of dewatering features such as pipes, dikes, pillars, and dish structures (Lowe, 1982); and (4) Debris flows: commonly consisting of conglomerates, breccias, and megabreccias occurring in thick sequences that are poorly sorted with chaotic bedding. These deposits are found both on high- and low-angle slopes either on the slope or distally into the basin (Cook, 1983). According to previous studies of relationships of resedimented carbonate materials, the stacking of flow types can be used to infer the distance from the shelf and declivity of the slope (Enos and Moore, 1983). These distances are based on the energy and viscosity of the flow which may be inferred by sedimentary structures and presence or absence of a cohesive matrix that can act to prevent frictional forces from retarding the flow (Figure 16).

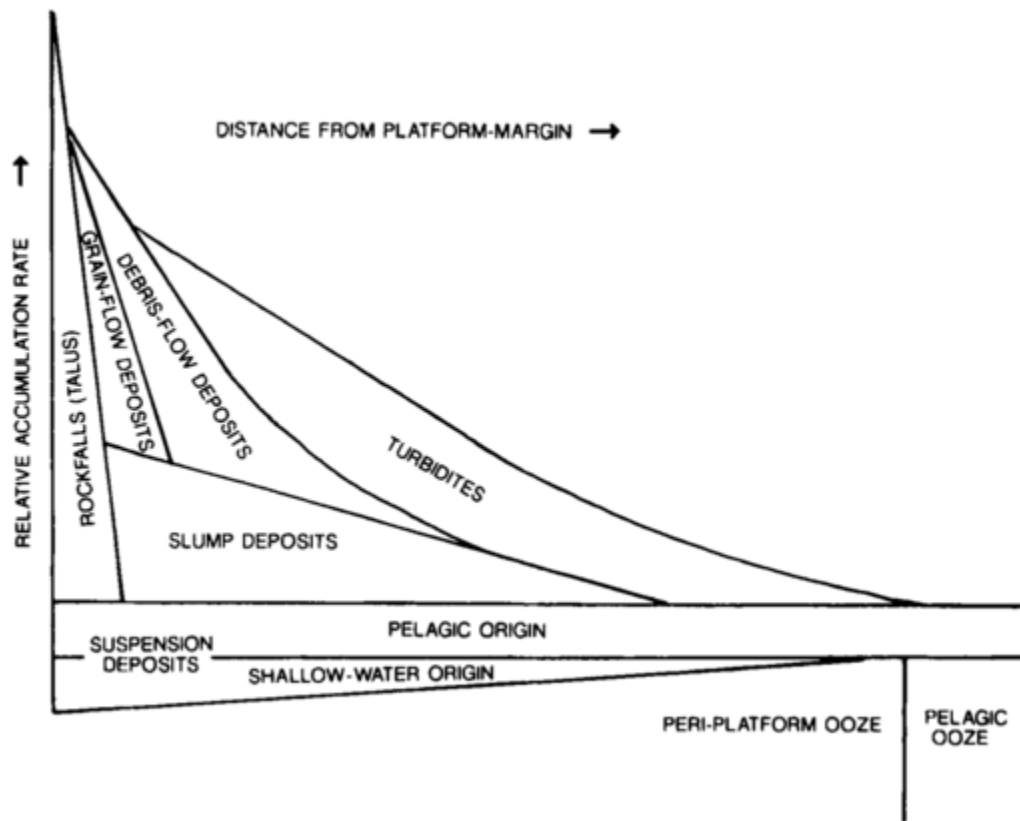


Figure 16. Diagram representing types of resedimented carbonate debris versus distance from platform source (Enos and Moore, 1983).

DEPOSITIONAL FACIES

On the basis of lithology, texture, and structures of observed core material, depositional facies have been designated in order to characterize the type of gravity flow and estimated distance from the shelf margin.

Turbidite Facies

Turbidites containing Bouma Sequence units B, D, and E occur overlying porous packstone to grainstone facies. Horizontal and wavy, thinly-laminated organic-rich carbonate mud dominates with interbeds of skeletal wackestone near the base. Wackestone is primarily shelf-derived fossils including fusulinids, crinoids, and brachiopod fragments set in a dark, organic-rich matrix of mud. Fining upward from wackestone to mudstone is common, along with scouring at the base of flow units. The turbidite facies also includes the occasional convolute laminae and soft sediment deformation in mudstone, with preservation of ripples at the base of massive mudstone, suggesting working of sediment by the action of deep currents during periods of quiescence. Bedding is predominately horizontal but is preceded by higher angle surfaces to a maximum angle of 45° at the base of some flows. This change in declivity from high to lower angle is interpreted to represent a deepening of the basin where the sediments transition

from erosion and bypassing the slope to a draping of sediments out of suspension. Although core samples are absent in the bulk of the middle of the Wolfcamp Shale, at the top of the Wolfcamp Shale, horizontally laminated mudstones are encountered before transitioning into the lower Leonard Limestones.

These deposits would represent deposition of sediments at the greatest distance from the shelf margin and their presence in the study area is likely representative of increased accommodation space and a southwestern retreat of the platform margin during a transgressive systems tract.

Grain Flow Facies

The deepest cored deposits in the Wolfcamp Reef interval consist of thick bedded to massive grainflow facies consisting of silt to coarse-sand sized lithoclasts and bioclasts. High angle contacts between flows indicate deposition on the slope and are occasionally interrupted by high angle shale breaks where mudstone is deposited between gravity flow events. Lithologies of grain flow facies are primarily lithoclast and bioclast packstone to grainstone and are often porous. Allochems in the grainflow facies range from clearly skeletal material consisting of tubular foraminifera, crinoids, brachiopod and bivalve fragments, bryozoans, and algal material, to less distinct allochems that have experienced

extensive alteration through micritization of grains and destruction of original material. Porosity is both intra- and intergranular with radial calcite spar cement. These allochthonous sediments are inferred to have originated either on or proximal to the shallow platform environment during sea level highstands, when carbonate production outpaced sea-level on the windward side of the platform and thick deposits of carbonate sand were shed into the lower basin. Grainflows lack a muddy matrix, and the likely mechanism of transport is grain to grain interaction where frictional forces will quickly retard the flow.

Debris Flow Facies

Debris flow facies found in the Simpson Canyon cores are located between the grain flow and turbidite facies at the top of the Wolfcamp Reef interval. The debris flows consist of lithoclast rudstones (Embry and Klovan, 1971) as large as 4 inches in diameter with a bioclast wackestone or mudstone matrix. Lithoclasts are composed of bioclast packstones, grainstones, and algal boundstones. Packstones and grainstones contain abundant benthic foraminifera, brachiopod and bivalve fragments, crinoid plates and columnals, and fenestrellina bryozoans. Algal boundstones contain phylloidal algae, tubiphytes, halimeda plates and encrusting forams with a micrite infilling. The presence of these binding organisms implies carbonate mounds that underwent

failure, interpreted to occur during lowstands as steep canyons were being cut into the margin. Although the conglomeratic clasts are large, the presence of a lubricating matrix indicates transport distances that would exceed those lacking a matrix.

Stratigraphic Relationships

The relationships exhibited by these gravity flows are shown in cross section (Figure 17) where the lowermost deposits consist of thick and continuous grain flows. These deposits are referred to as the Wolfcamp “Reef” section in literature due to the clean gamma ray signature although they are recognized along the eastern margin of the central basin platform as allochthonous grains with a shallow water platform origin (Hobson et. al., 1985). Although wireline logs often do not penetrate through the entire grain flow facies, where they do, the deposits thicken basinward. This same basinward thickening and similar wireline log character is seen in the lowest Leonard deposits above the top of the Wolfcamp Shale which is used as a datum due to its easily recognized log character and continuous nature. This suggests another cycle of highstands shedding of platform material and renewed progradation of the platform margin.

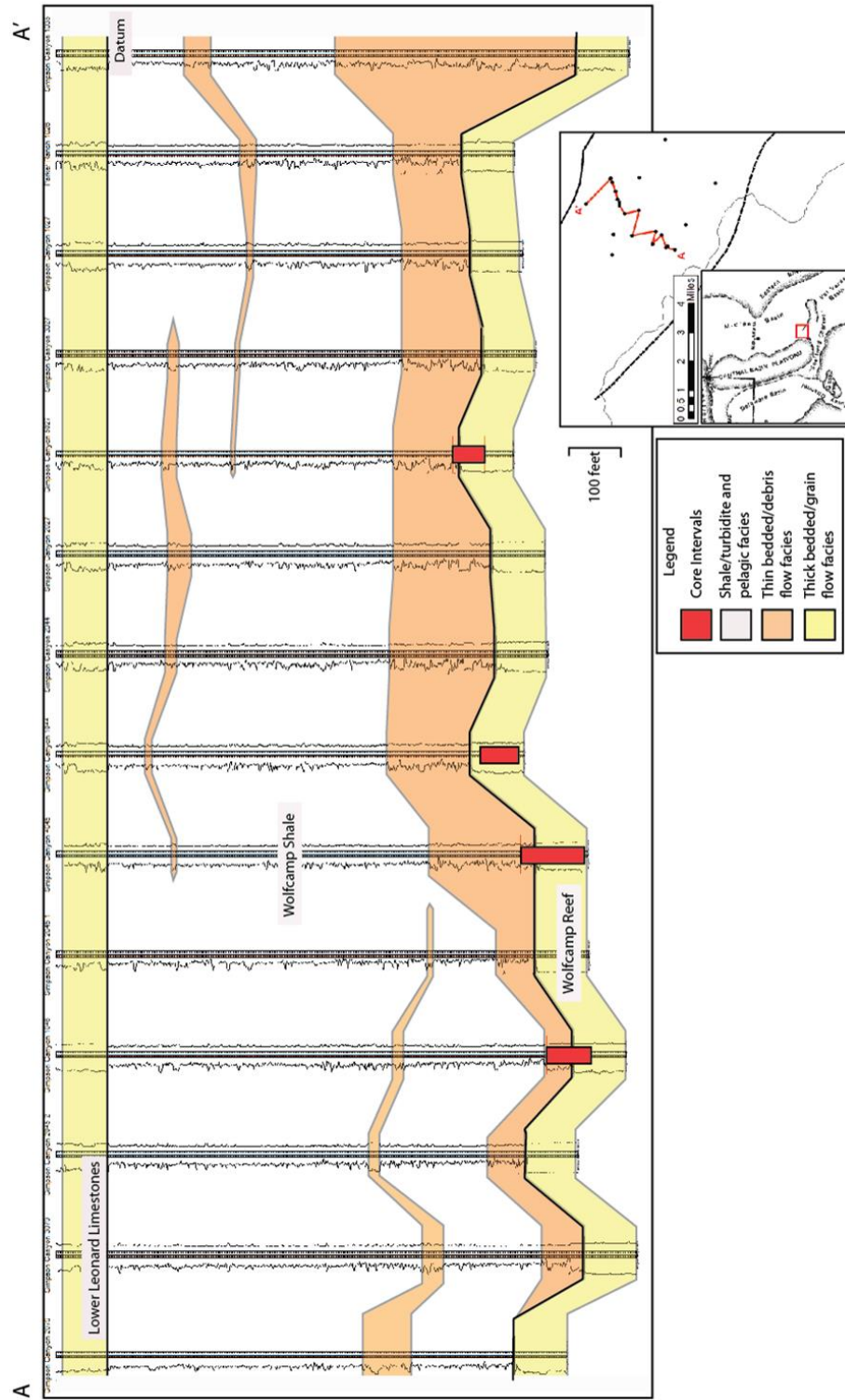


Figure 17. Stratigraphic cross section along dip through the study area illustrating log/depositional facies relationships and the location of cored intervals. Datum is the top of the Wolfcamp Shale.

Deposited above the grain flow facies is the debris flow facies interbedded with turbidites and hemipelagic mudstones. Debris flows exhibit a log response of mixed high and low gamma signatures and appear to have a generally upward fining log character with multiple cycles of sedimentation as failure took place on the margin. Debris flows also thicken basinward; however, these deposits appear to have multiple pulses of backwards rotational geometry characteristic of a thick plug at the front of the flow that prevents flow further into the basin so that subsequent flows backfill behind older flows until the topography is filled in. The debris flow morphology of single flows and multiple stacked flows are illustrated in Figure 18. Between flows, either pelagic sedimentation, settling of finer material re-entrained during flow, or turbidite flows deposit fine grained sediments that exhibit a high gamma response.

Due to the high energy required to transport the large clasts contained in the debris flow facies, it is interpreted that during lowstands, incision of the shelf margin created over steepened canyons which were prone to failure. This failure produced an increase in accommodation space and would indicate a backstepping of the platform margin. Also, deposits with similar log responses exhibit a retrogradational pattern as lobes of debris flows found in the overlying finer grained facies are deposited increasingly closer to the platform margin at the southwest of the study area. Failure on the margin brought large blocks of lithoclast rudstone and algal boundstone to deeper portions of the basin

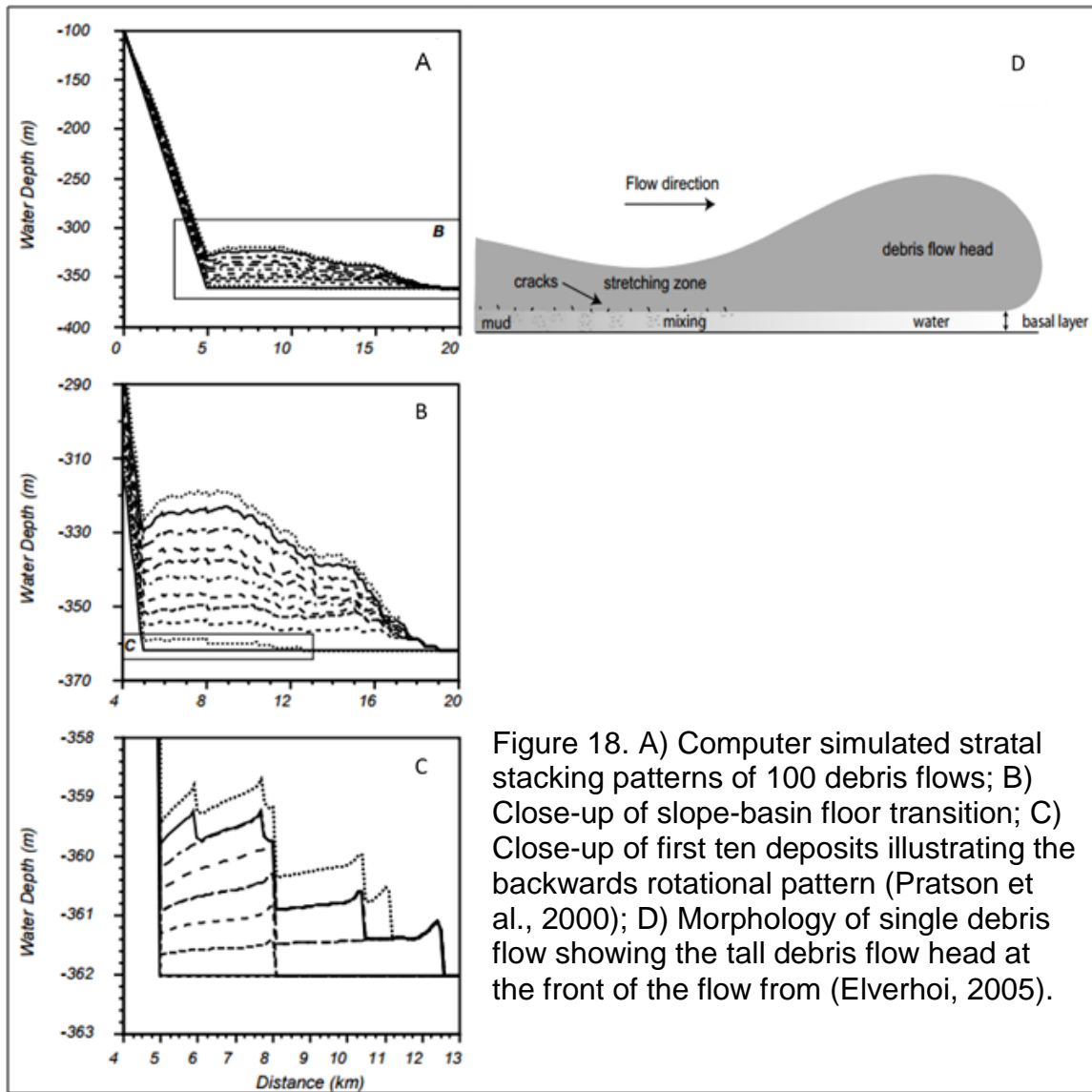


Figure 18. A) Computer simulated stratal stacking patterns of 100 debris flows; B) Close-up of slope-basin floor transition; C) Close-up of first ten deposits illustrating the backwards rotational pattern (Pratson et al., 2000); D) Morphology of single debris flow showing the tall debris flow head at the front of the flow from (Elverhoi, 2005).

as far 5 miles from the marginal edge of the study area and continued to do so during higher frequency cycles of transgression and regression. The great distance that these larger clasts traveled is likely due to the lubricating matrix of fine muds that prevented the flow from freezing due to frictional forces.

At the base of the overlying Wolfcamp Shale lies the fine-grained distal turbidite and pelagic sedimentation deposits that exhibit a characteristically high gamma response and appear to drape over the coarser-grained deposits below. The turbidite deposits are interbedded with allochthonous carbonate debris along with laminated mudstone and shale that settled out of suspension. Although the log character of the distal turbidites and the laminated quiet water deposits have a very similar log character, in core the fine grained sediments deposited by suspension can be distinguished from turbidite flows by the presence of fine laminations and the lack of basal scour surfaces. Often, the turbidite flows will present a high angle scour surface at their base instead of draping over the underlying deposits along with having occasional thin layers of allochthonous grains at an angle.

Lastly, fine-grained, quiet water deposition of horizontally bedded shale with thin carbonate mudstone laminae dominates the slope until lower Leonard carbonate grain flows are encountered. The various types of gravity flows encountered in the area have been primarily characterized based on the dip

section seen in figure 17. Although this is useful for observations of flow character in two dimensions, a determination of whether these flows are confined or not require an analysis of the sediments along strike such as in figure 19. In this strike section, a lack of defined channels is observed; however, this is likely due to sparse well control and not the absence of channels.

Lastly, although little core data is present in this interval of the Wolfcamp Shale, log calibrations with shale rich core indicates that massive shale dominates the upper Wolfcamp and represents a deepening of the basin during a transgressive systems tract where up to 700 feet of fine-grained, high gamma response deposits are found. Towards the platform margin, carbonate beds with a maximum thickness of 30 feet appear in the shale and can be traced basinward. These beds do not extend as far into the basin as the underlying allochthonous carbonates, and are likely grain flows being shed from a backstepping platform margin during transgression, as they extend less and less into the basin with each deposit. Wolfcamp deposition in the study area is punctuated with the renewed deposition of thick-bedded carbonates in the lower Leonard, which exhibits a log character similar to the lowermost Wolfcamp Reef sediments of allochthonous grain flow deposits. This coincides with a return to highstands near the end of a first order sequence, which marks the end of the Wolfcampian and the beginning of the Leonardian (Figure 4).

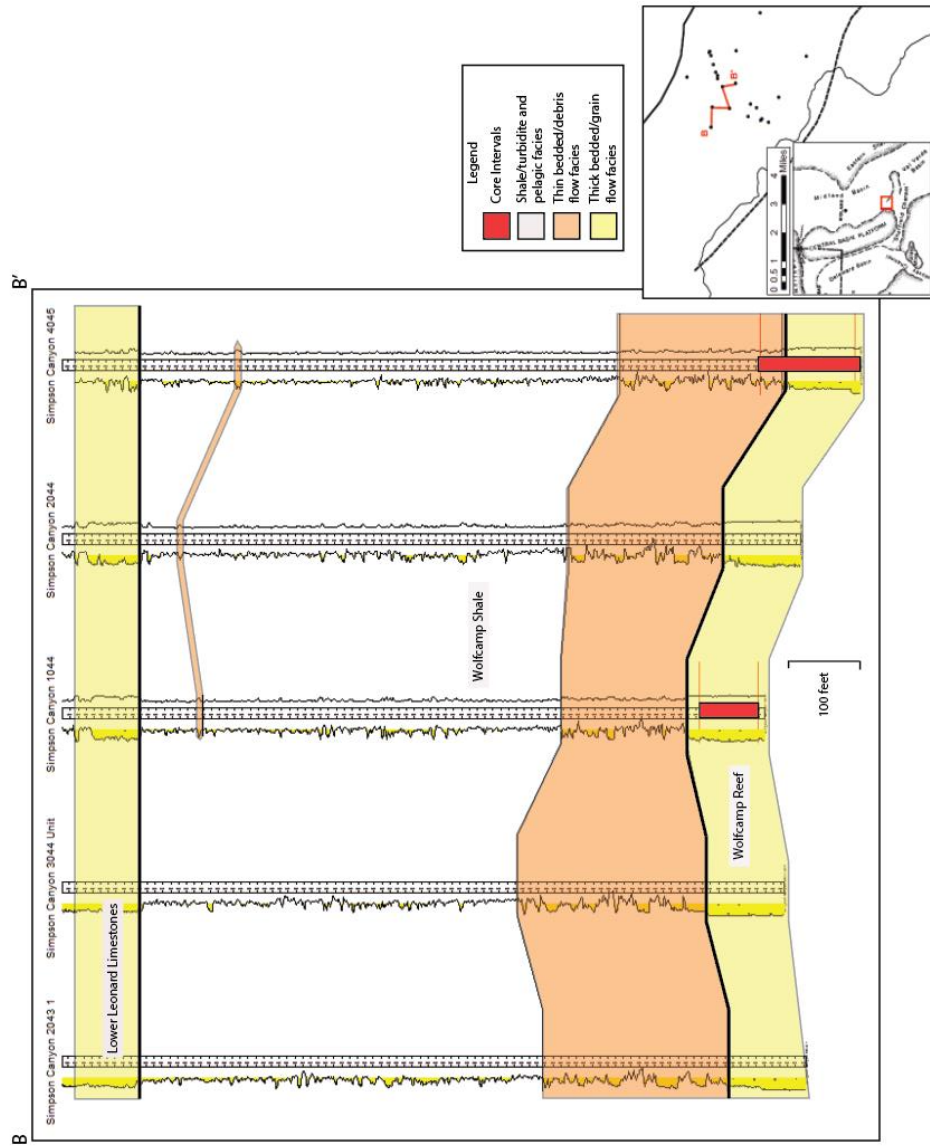


Figure 19. Stratigraphic cross section along strike through the study area illustrating log/depositional facies relationships and the location of cored intervals. Datum is the top of the Wolfcamp Shale.

LITHOFACIES INTERPRETATION

Interpretation of underlying sediments is difficult due to lack of core samples and the low amount of well logs that penetrate deeper than the Wolfcamp “Reef” deposits. Previous studies on the Wolfcamp in both the southern Midland Basin and on the southern Central Basin Platform indicate that Wolfcamp deposition overlies Upper Pennsylvanian Canyon and Cisco formations (Figure 20). During Canyon and Cisco deposition, glacio-eustatic sea level fluctuations similar to the Pleistocene glaciations resulted in high amplitude sea level rise and fall on the scale of 150-300 feet every 110,000 years (Saller, 2014). These sea level fluctuations would drown and expose platform limestones, which would either deposit limestones on the platform during sea level highs or during sea level lowstands, the platform would be subaerially exposed and rivers would transport siliciclastic material to the slope and basin.

This is represented in the study area by a detrital log signature in the photoelectric tool beneath the overlying Wolfcamp “Reef” carbonate grain flows. Better constrained deposits overlie the detrital Canyon and Cisco slope and basin sediments and include cored intervals of the Wolfcamp “Reef” allochthonous grain and debris flows, Wolfcamp Shale distal turbidites and basinal shales, and finally the Lower Leonard Limestones.

<i>SERIES</i>	<i>MID-CONTINENT STAGE</i>	<i>WEST TEXAS FORMATION</i>
LOWER PERMIAN	LEONARDIAN	LEONARD
	WOLFCAMPIAN	WOLFCAMP
PENNSYLVANIAN	286 ± 6 m.y. VIRGILIAN	CISCO
	MISSOURIAN	CANYON
	296 ± 5 m.y. DES MOINESIAN	STRAWN
	ATOKAN	ATOKA
	MORROWAN	MORROW
320 ± 10 m.y.		

Figure 20. Stratigraphic column on the eastern Central Basin Platform from Saller et al., 1994.

Wolfcamp “Reef” sediments are only cored at the top of the formation so that the exact nature of the contact between the Cisco Formation is unknown; however, this shift from detrital sedimentation to massive carbonate packstone and grainstone is likely to represent a shift from lowstands in the Cisco, to a starved basin during the subsequent transgression, and highstands shedding during early Wolfcamp that deposited thick sequences of packstone to grainstone on the slope. The interpretation of highstand shedding of sediments that originated on the platform is based on the similar lithology of grainstones and packstones that were not shed into the slope and basin in more northern regions (Saller et al., 1994).

Although the platform sediments are similar, the study by Saller et al. (1994) in Andrews County exhibit extensive evidence of subaerial exposure and lack the interbedded basinal shale and mudstone like the sediments encountered in the Simpson Canyon study area. These sediments are the fine to coarse grained sand-sized allochems that experienced micritization in the photic zone by endolithic algae. These grains were rounded by the action of relatively high energy waves breaking on the windward side of the Central Basin Platform before they could be cemented and fully lithified. Sediments were later driven off by the action of those waves or storms that deposited them in the slope to basinal environment in which they are found in the study area, likely as channels and sheets of material that followed declivities in the slope or between

topography from previous gravity flows. Higher frequency cycles of sea level fluctuations are likely responsible for the pulses of grain flow deposition in the study area. The periods of quiescence between flows are marked by the presence of laminated black shales. Due to the relatively sparse distribution of core samples and the chaotic stratigraphy of individual grain flow events, these cycles cannot be tracked throughout the study area.

After deposition, sparry calcite cement occluded most of the pore space between grains and burial pressure resulted in the deformation of grains along with the development of stylolites at boundaries between individual flows. Later, both interparticle and intraparticle porosity developed as undersaturated fluids dissolved cement and unmicritized portions of the grains. Distribution of porosity is massive in core but is laterally heterogeneous and cannot be tracked throughout the study area.

As sea level fell, ramp margin mounds of binding organisms such as tubiphytes, bryozoans, encrusting foraminifera, phylloidal algae, and halimeda were eroded off of the slope along with lithified packstones and grainstones as incising canyons created high angle slopes prone to failure. The deposits during this time in the study area represent the basinward equivalent of the subaerial exposure on the shelf where a Mid-Wolfcampian unconformity has been recognized in platform environments (Fu, Q., 2011). These debris flows were transported to slope and basin settings where the resultant material is recognized

in the core as the lithoclast rudstone to floatstone and compose the carbonate rich material in the thin-bedded log facies.

During transport, the debris flows likely disturbed fine-grained material which was incorporated into the flows and acted as the lubricating matrix. Debris flows during transport are known to erode material from the substrate due to the high energy required to move such large particles. Debris flows also have a characteristic form to the flows where a tall plug travels at the head of the flow, and when the flow freezes, the thick plug acts a barrier to contain subsequent flows until the topography is filled in with a backwards rotational pattern.

After deposition, compressional effects from burial sutured lithoclasts together with stylolites where matrix is lacking, resulting in a destruction of clast boundaries that impart a brecciated appearance. Where matrix is present, the lithology is dark, muddy material with loose lithoclasts and bioclasts and stylolites are lacking. These zones of matrix show that lithoclasts in the rudstone facies are moderately rounded due to transport from the ramp margin. Abundant vertical fractures are found in these sediments that cross through grains, indicating that they formed after resedimentation. Above the debris flows, finer grained turbidity currents are found, with an origin that is likely related to erosion of muddy substrate during the debris flow events.

With sea level rise, fine-grained transgressive sediments begin draping over the underlying coarser grained debris flows and turbidites. This was a period

of backstepping for the platform margin where the low gradient ramp morphology and lack of platform rim was conducive to a landward shift of facies. During this period, thick, basinal Wolfcamp Shale was deposited in a deepening basin and the resulting sediments are thinly laminated, organic-rich, black shales and mudstones. Higher frequency cycles during this period resulted in the shedding of carbonate debris from the platform margin into the slope and basin as gravity flow deposits. These are recognized as relatively thin deposits of low gamma ray response carbonate sediments that are laterally continuous between wells. These debris flows extend into the basin as increasingly proximal deposits that aid in the interpretation of a backstepping trajectory of the platform margin. Finally, as sea level once again reached a highstand, carbonates began prograding across the Wolfcamp Shale deposits. These Lower Leonardian limestones represent the last deposits encountered in the study area and coincide with a shift of environment from humid to arid as carbonate volume decreases and siliciclastics and evaporites begin to dominate the Permian basin.

EXPLORATION CONSIDERATIONS

Reservoir facies in the Simpson Canyon area are the porous packstone to grainstone lithofacies deposited as grain flows during sea level highstands. Maximum estimated porosities of 13 percent are massive in individual cores but cannot be traced laterally between wells. The closest analogue reservoirs are located on the opposite side of the Central Basin Platform slope in Pecos County, Texas at Nuz, Hokit North, and Hokit Northwest fields (Carlisle, 2003). The reservoir zones in this area are known to have high permeabilities up to 2 darcies; however, lateral heterogeneity is unpredictable as offset wells are often found to have poor reservoir quality. In the Wolfcamp “Reef” grainstone reservoir, compartmentalization is known to occur due to different reservoir pressures throughout the fields in question. Total production in the three fields through December 1996 was reported to be 16.7 BCFG and 384 MBO. Overall, exploration in the study area would be difficult due to the remote nature of the area, rapid elevation changes and rugged topography, and the lack of roads. The report by Carlisle (2003) over the analogue fields states that the variability in the gas oil ratio, reservoir pressures, and hydrogen sulfide content make the Wolfcamp “Reef” play a challenging project.

Aside from reservoirs directly encountered in the study area, the recognition of the types of gravity flows and their sequence stratigraphic

implications may have an impact on sediments found both on the platform and into the deeper basin. The slope environment, in which this study takes place, acts as the transition between the two areas and may give insight into patterns of sedimentation and location of reservoirs in both. For instance, recognition of debris flows on the slope could indicate that lowstand conditions were prevailing and the coeval sediments on the slope would be undergoing exposure and possible karstification. These exposure conditions in areas such as the Parker, Andrews, and Deep Rock fields in Andrews County, Texas have been known to generate extensive reservoir grade porosity (Saller et al., 1994). Conversely, during periods of sea level lowstands when debris flows and turbidites are deposited on the slope, runout of carbonate debris for tens of miles could be supplying carbonate material to the deep Wolfcamp Shale in the Midland Basin where carbonate rich shales often serve as frac barriers or indicate periods of poor organic preservation and low TOC (total organic carbon) in unconventional reservoirs (Baumgardener and Hamlin, 2014).

CONCLUSION

Although platform margin slope to basin environments have experienced relatively little study aside from proprietary endeavors, these transitional sediments have the capability to act as both reservoirs along with indicators of how sea level changes transfer material throughout the environment. The subaqueous carbonate gravity flows encountered in the Simpson Canyon area record a history of platform margin progradation, collapse, and retrogradation through the sediments encountered in the Simpson Canyon cores. Through the relationships of grains to matrix and visible structures found in the core, mechanisms of transport are inferred and used to determine the type of gravity flow encountered.

Grain flows, debris flows, and turbidites all represent downslope movement of carbonate material but vary in their capability to travel large distances so that when encountered, distance from the platform edge can be inferred. This, along with the determination of the origin of the sediment, allows the material in core to be placed within a sequence stratigraphic framework. In the Simpson Canyon study area, highstand bioclast packstone to grainstone grain flows in the Wolfcamp "Reef" division underlie falling stage to lowstand carbonate conglomerate debris flows. Algal boundstone lithoclast present in the debris flows hint at incision and failure of the shelf edge. These debris flows form

the base of the Wolfcamp Shale division and are increasingly interbedded with turbidites and pelagic shales during the subsequent sea level transgression. Thick transgressive shales are deposited as the backstepping shelf edge retreated from the study area until highstands grain flows of the lower Leonard limestones advance into the study area. Additionally, although the interpretation given in this study may be simplistic, it acts to fill in a gap in the knowledge of how the southern Central Basin Platform slope environment has evolved through the Early Permian.

FUTURE WORK

Further work on this area could utilize geochemical signatures to identify nuances in the Wolfcamp Shale that is hidden from macroscopic observation, along with biostratigraphic work to fully constrain the age of the resedimented material. Continuation of the work completed in this study would be aided by well control moving both further into the basin and onto the platform.

REFERENCES

- Adams, D. C., and Keller, G. R., 1996, Precambrian Basement Geology of the Permian Basin Region of West Texas and Eastern New Mexico: A geophysical Perspective, AAPG Bulletin, V. 80, No. 3, p. 410 – 431.
- Adams, E. W., and Kenter, J. A. M., 2013, So Different, Yet So Similar: Comparing and Contrasting Siliciclastic and Carbonate Slopes, SEPM Special Publication No. 105, p. 14-25.
- Adams, J. E., 1965, Stratigraphic-Tectonic Development of Delaware Basin, AAPG Bulletin, Vol. 49, No. 11, p. 2140 – 2148.
- Baumgardener, R. W., and Hamlin, H. S., 2014, Core-based Geochemical Study of Mudrocks in Basinal Lithofacies in the Wolfberry Play, Midland Basin, Texas, Part II, Search and Discover Article #10572.
- Candelaria, M. P., Sarg, J. F., and Wilde, G. L., 1992, Wolfcamp Sequence Stratigraphy of the Eastern Central Basin Platform, in Mruk, D. H., and Curran, C., eds., Permian Basin exploration and production strategies: application of sequence stratigraphic and reservoir characterization concepts: West Texas Geological Society Publication 92-91, p.27–44.
- Carlisle, P. H., 2003, The Attributes of a Wolfcamp “Reef” Play Pecos Co., TX, AAPG Southwest Section Convention, Fort Worth, Texas, March 5th, 2003, pp. 16.
- Chernykh, V.V., and Ritter, S.M., 1997, Streptognathodus (Conodonta) Succession at the Proposed Carboniferous-Permian Boundary Stratotype Section, Aidaralash Creek, Northern Kazakhstan: Journal of Paleontology, p. 459-474.
- Cook, H. E., 1983, Ancient Carbonate Platform Margins, Slopes and Basins, SEPM Special Publication: Platform Margin and Deep Water Carbonates (SC12), pp. 189.
- Dunham, R. J., 1962, Classification of Carbonate Rocks According to Depositional Texture, Classification of Carbonate Rocks – A Symposium, p. 108 – 121.

- Elverhoi, A., Issler, D., De Blasio, F. V., Ilstad, T., Harbitz, C. B., and Gauer, P., 2005, Emerging Insights into the Dynamics of Submarine Debris Flows, Natural Hazards and Earth System Sciences, European Geosciences Union, Vol. 5, p. 633-648.
- Embry, A. F., and Klovan, J. E., 1971, Upper Devonian Stratigraphy, Northeastern Banks Island, N.W.T., Bulletin of Canadian Petroleum Geology, Vol. 19, No. 4, p. 705-729.
- Enos, P., and Moore, C. H., 1983, Fore-reef Slope Environment: Chapter 10, Special Publication: Memoir 33: Carbonate Depositional Environments, p. 507-537.
- Ewing, B. T., Watson, M. C., McInturff, T., and McInturff, R. N., 2014, The Economic Impact of the Permian Basin's Oil and Gas Industry, Permian Basin Petroleum Association Report, Midland, Texas, August 2014, p. 49-50.
- Ewing, T. E., 2013, Three Scales of Late Paleozoic Structures in the West Texas Basin – Description and Genesis, AAPG Search and Discovery Article No. 30273.
- Flamm, Douglas S. 2008, Wolfcampian Development of the Nose of the Eastern Shelf of the Midland Basin, Glasscock, Sterling, and Reagan Counties, Texas, Department of Geological Sciences Master's Thesis. Brigham Young University. p. 1-54.
- Fu, Q., 2011, A Synthesis of the Wolfcampian Platform Carbonate System in the Permian Basin Region, West Texas Geological Society Presentation.
- Hamlin, H. S., 2009, Ozona Sandstone, Val Verde Basin, Texas: Synorogenic Stratigraphy and Depositional History in a Permian Foredeep Basin, AAPG Bulletin, V. 93, No. 5, p. 573 – 594.
- Haq, B.U., and Shutter, S.R., 2008, A Chronology of Paleozoic Sea-level Changes: Science, v. 322, October 2008, p. 64-68.
- Hobson, J. P., Caldwell, C. D., and Toomey, D. F., 1985, Early Permian Deep-Water Allochthonous Limestone Facies and Reservoir, West Texas, AAPG Bulletin V. 69, No. 12, p. 2130 – 2147.

- Hobson, J. P., Caldwell, C. D., and Toomey, D. F., 1985, Sedimentary Facies and Biota of Early Permian Deep-water Allochthonous Limestone, Southwest Reagan County, Texas, The Society of Economic Paleontologists and Mineralogists (SEPM): Deep-Water Carbonates, p. 93-139.
- Kerans, C., Playton, T., Phelps, R., and Scott S. Z., 2013, Ramp to Rimmed Shelf Transition in the Guadalupian (Permian) of the Guadalupe Mountains, West Texas and New Mexico, SEPM Special Publication No. 105, p.26-49.
- King, P. B., 1942, Permian of West Texas and Southeastern New Mexico, AAPG Bulletin Vol. 26, p. 535 – 763b.
- Loucks, R. G., Brown, A. A., Achauer, C. W., and Budd, D. A., 1985, Carbonate Gravity-Flow Sedimentation on Low-Angle Slopes Off the Wolfcampian Northwest Shelf of the Delaware Basin, SEPM Special Publication: Deep-Water Carbonates (CW6), pp. 37.
- Lowe, D. R., 1982, Sediment Gravity Flows: II. Depositional Models with Special Reference to the Deposits of High-density Turbidity Currents, Journal of Sedimentology, Society of Economic Paleontologists and Mineralogists, v. 52, p. 279-297.
- Mazzullo, S. J., and Reid, A. M., 2012, Lower Permian Platform and Basin Depositional Systems, Northern Midland Basin, Texas, Controls on Carbonate Platform and Basin Development, SEPM Special Publication No. 44, pp. 16.
- Mazzullo, S. J., 1997, Stratigraphic Exploration Plays in Ordovician to Lower Permian Strata in the Midland Basin and on the Eastern Shelf, in W. D. DeMise, ed., Permian basin oil and gas fields: Turning ideas into production: West Texas Geological Society Publication 97-102, p. 1–37.
- Middleton, G. V., and Hampton, M. A., 1976, Subaqueous Sediment Transport and Deposition by Sediment Gravity flows, in Stanley, D. J., and Swift, D. J. P., eds., Marine Sediment Transport and Environmental Management: New York, Wiley, p. 197-218.
- Mullins, H. T., & Van Buren, H. M., 1979, Modern Modified Carbonate Grain Flow Deposit, Journal of Sedimentary Petrology, Vol. 49, No. 3, p. 747 – 752.

- Pratson, L. F., Imram, J., Parker, G., Syvitski, J. P. M., and Hutton, E., 2000, Debris Flows vs. Turbidity Currents: a Modeling Comparison of Their Dynamics and Deposits, in A. H. Bouma and C. G. Stone, eds., *Fine-grained Turbidite Systems*, AAPG Memoir 72/SEPM Special Publication 68, p. 57-72.
- Ritter, S.M., 1995. Upper Missourian-lower Wolfcampian (upper Kasimovian-lower Asselian) conodont biostratigraphy of the midcontinent, USA: *Journal of Paleontology*, p. 1139-1154.
- Ross, C. A., 1963, *Standard Wolfcampian Series (Permian)*, Glass Mountains, Texas, Memoir - Geological Society of America, pp. 230.
- Saller, A., 2014, Late Pennsylvanian and Early Permian Sedimentation on the Central Basin Platform and Implications to the Wolfberry Deposition in the Western Midland Basin, Oral Presentation, Search and Discovery Article #10606.
- Sarg, J. F., Markello, J. R., and Weber, L. J., 1999, The Second-order Cycle, Carbonate-Platform Growth, and Reservoir, Source, and Trap Prediction, SEPM Special Publication No. 63, p. 11-34.
- Sellards, E. H., Adkins, W. S., and Plummer, F. B., 1932, *The University of Texas Bulletin: The Geology of Texas*, Vol. 1: Stratigraphy, Bureau of Economic Geology, p. 146-154.
- Sternbach, C. A., 2012, Petroleum Resources of the Great American Carbonate Bank, in *The Great American Carbonate Bank: The Geology and Economic Resources of the Cambrian – Ordovician Sauk Megasequence of Laurentia*: AAPG Memoir 98, p. 125 – 160.
- Tanos, C. A., Kupecz, J., Hilman, A. S., Ariyono, D., and Sayers, I. L., 2013, Diagenesis of Carbonate Debris Deposits from the Sebuk Block, Makassar Strait, Indonesia, *Proceedings, Indonesian Petroleum Association, 37th Annual Convention & Exhibition*, pp. 18.
- Udden, J. A., Baker, C. L., and Bose, E., 1916, *Review of the Geology of Texas: University of Texas Bulletin*, no. 44, p. 164.
- Udden, J. A., 1917, *Notes on the Geology of the Glass Mountains: University of Texas Bulletin*, 1753, p. 3-59.

Ward, R. F., Kendall, C., Harris, P. M., 1986, Upper Permian (Guadalupian) Facies and Their Association with Hydrocarbons – Permian Basin, West Texas and New Mexico, AAPG Bulletin, Vol. 70, p. 239-262.

Whalman, G. P., and Tasker, D. R., 2013, Lower Permian (Wolfcampian) Carbonate Shelf-margin and Slope Facies, Central Basin Platform and Hueco Mountains, Permian Basin, West Texas, USA, SEPM Special Publication No. 105, p. 305-333.

Yang, K., and Dorobek, S. L., 2012, The Permian Basin of West Texas and New Mexico: Tectonic History of a “Composite” Foreland Basin and its Effects on Stratigraphic Development, Stratigraphic Evolution of Foreland Basins, SEPM Special Publication No. 52, pp. 26.

APPENDIX

Well Name	API Number	Available Data
Simpson Canyon 4045	4210539639	Core, Well Logs
Simpson Canyon 1046	4210539584	Core, Well Logs
Simpson Canyon 5027	4210539889	Core, Well Logs
Simpson Canyon 1044	4210539658	Core, Well Logs
Simpson Canyon 1036	4210540041	Core
Simpson Canyon 2044	4210539794	Well Logs
Simpson Canyon 2027	4210539779	Well Logs
Simpson Canyon 2027	4210540875	Well Logs
Simpson Canyon 3027	4210539824	Well Logs
Parker Ranch 1026	4210540370	Well Logs
Simpson Canyon 3044	4210539912	Well Logs
Simpson Canyon 1078	4210539865	Well Logs
Simpson Canyon 1035	4210539954	Well Logs
Parker Ranch 2034	4210541121	Well Logs
Simpson Canyon 1076	4210539136	Well Logs
Simpson Canyon 2079	4210539224	Well Logs
Simpson Canyon 1	4210539073	Well Logs
Simpson Canyon 3079	4210539235	Well Logs
Simpson Canyon 2045 1	4210540743	Well Logs
Simpson Canyon 2045 2	4210539409	Well Logs
Simpson Canyon 2043	4210539840	Well Logs
Bouscaren 25	4210541347	Well Logs
Parker 30 1	4210541336	Well Logs

Figure A-1. Table detailing the wells used in the study along with the type of data available.

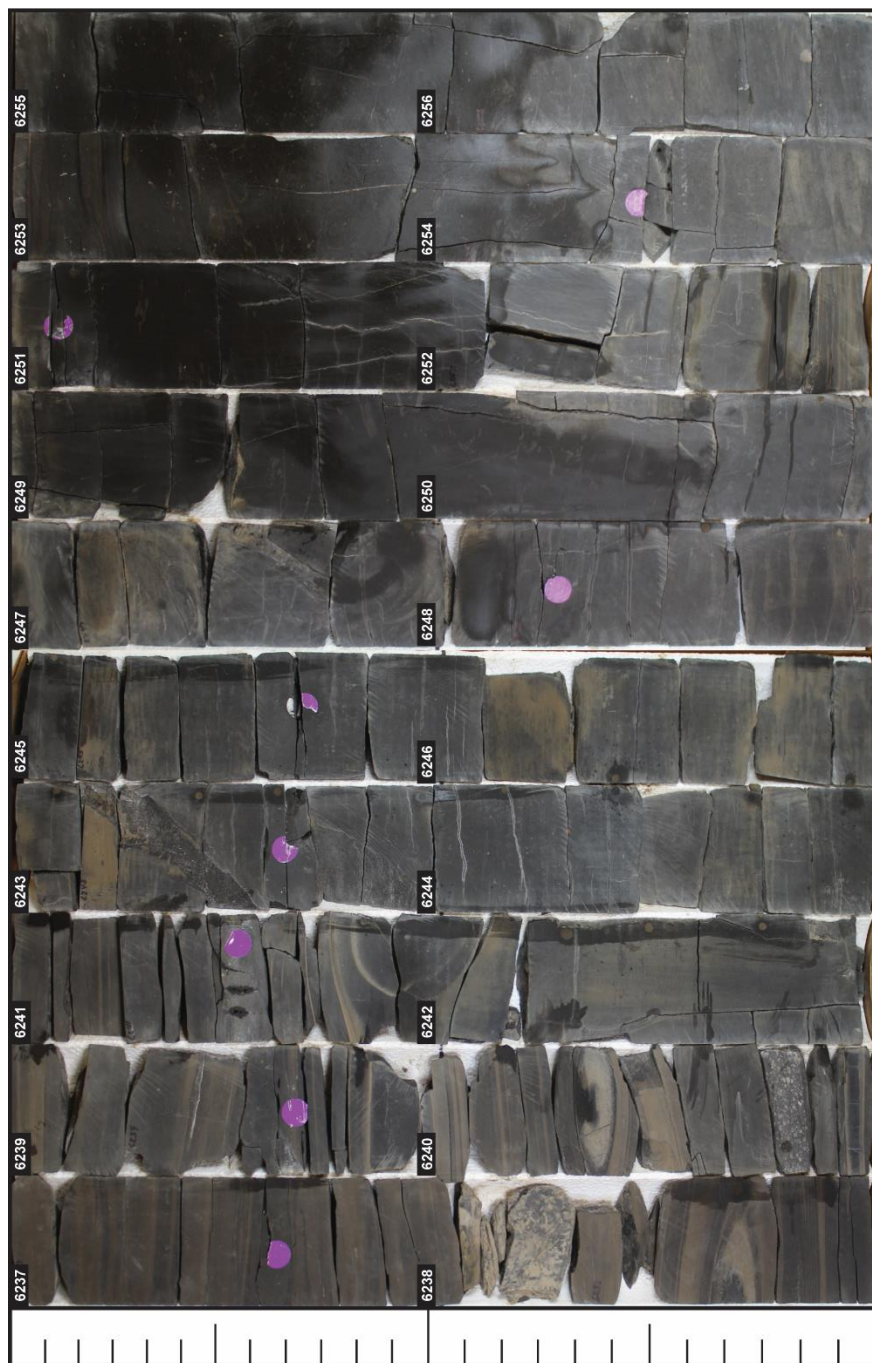


Figure A-2. Core image of Simpson Canyon 1036 interval 6237' to 6257'.

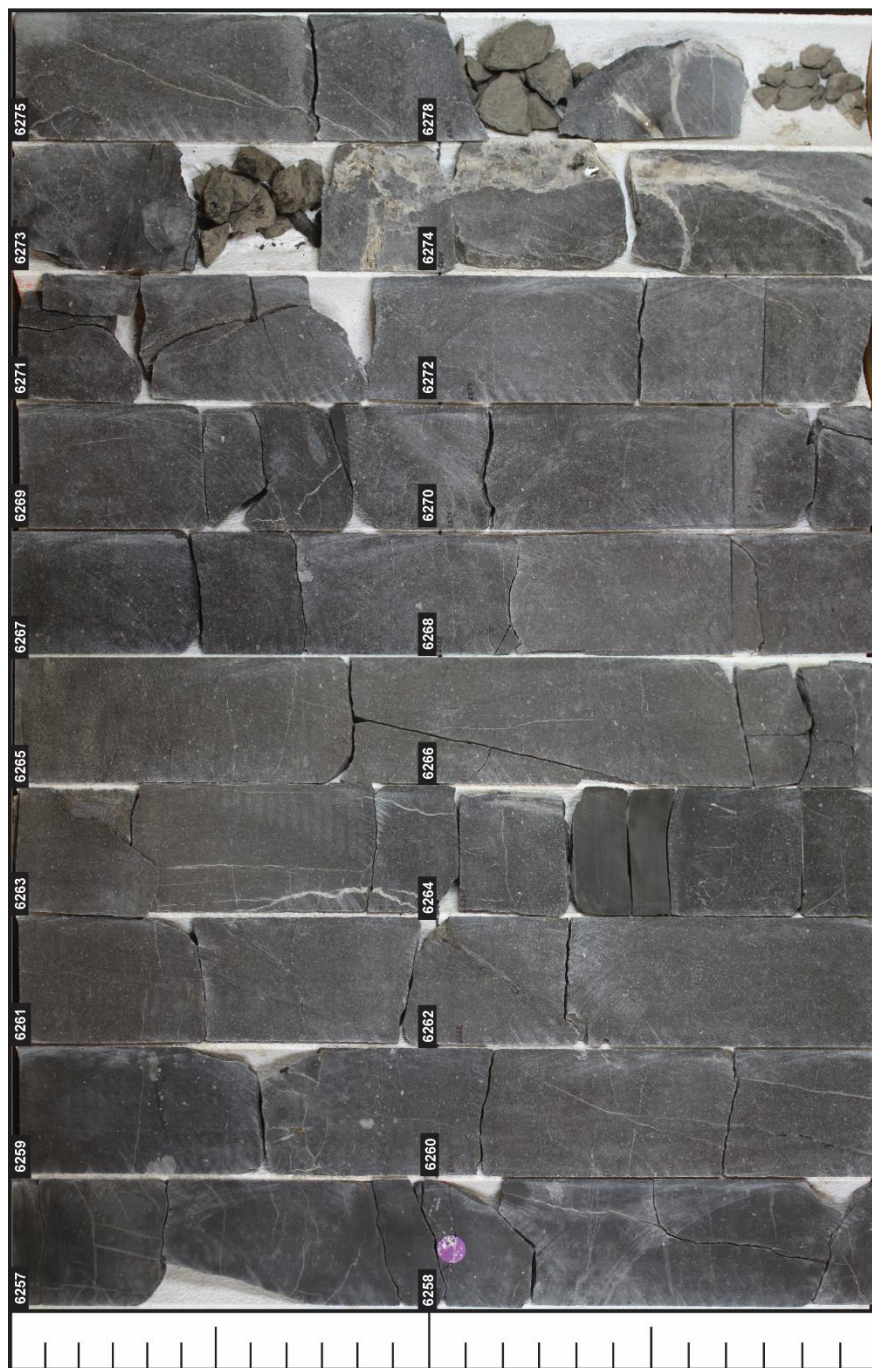


Figure A3. Core image of Simpson Canyon 1036 interval 6257' to 6279'.



Figure A4. Core image of Simpson Canyon 1036 interval 6279' to 6297'.

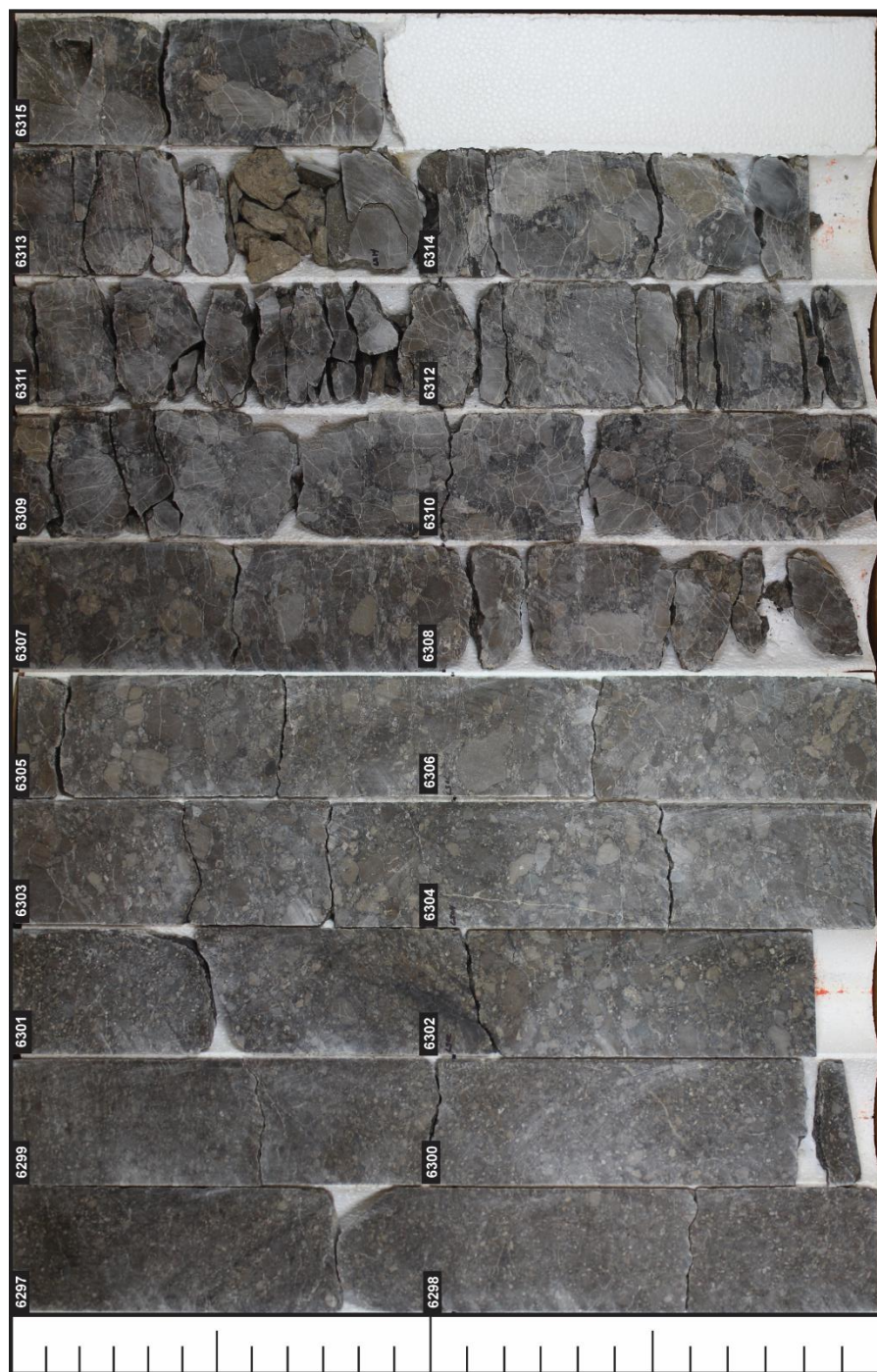


Figure A5. Core image of Simpson Canyon 1036 interval 6297' to 6216'.

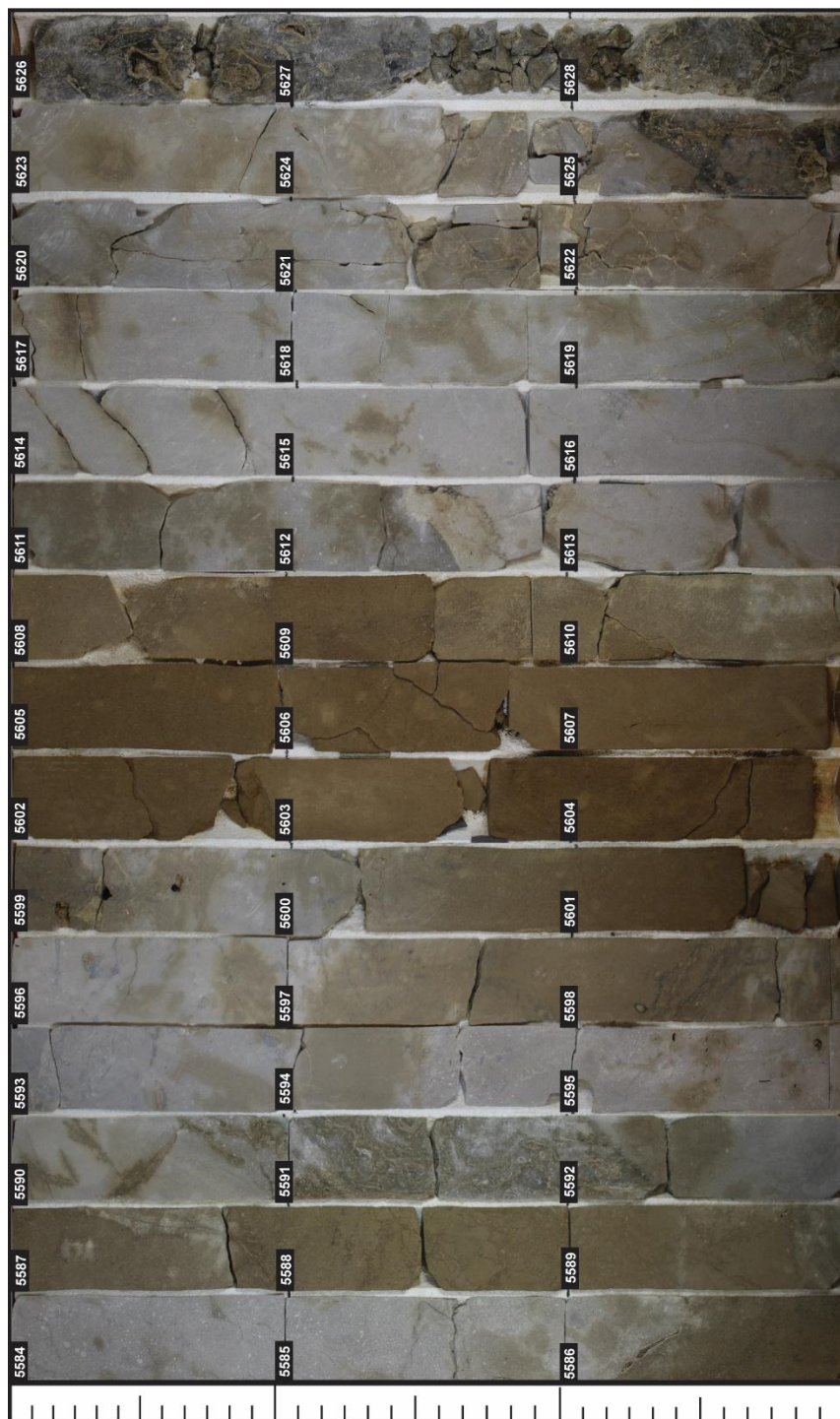


Figure A6. Core image of Simpson Canyon 1044 interval 5584' to 5629'.

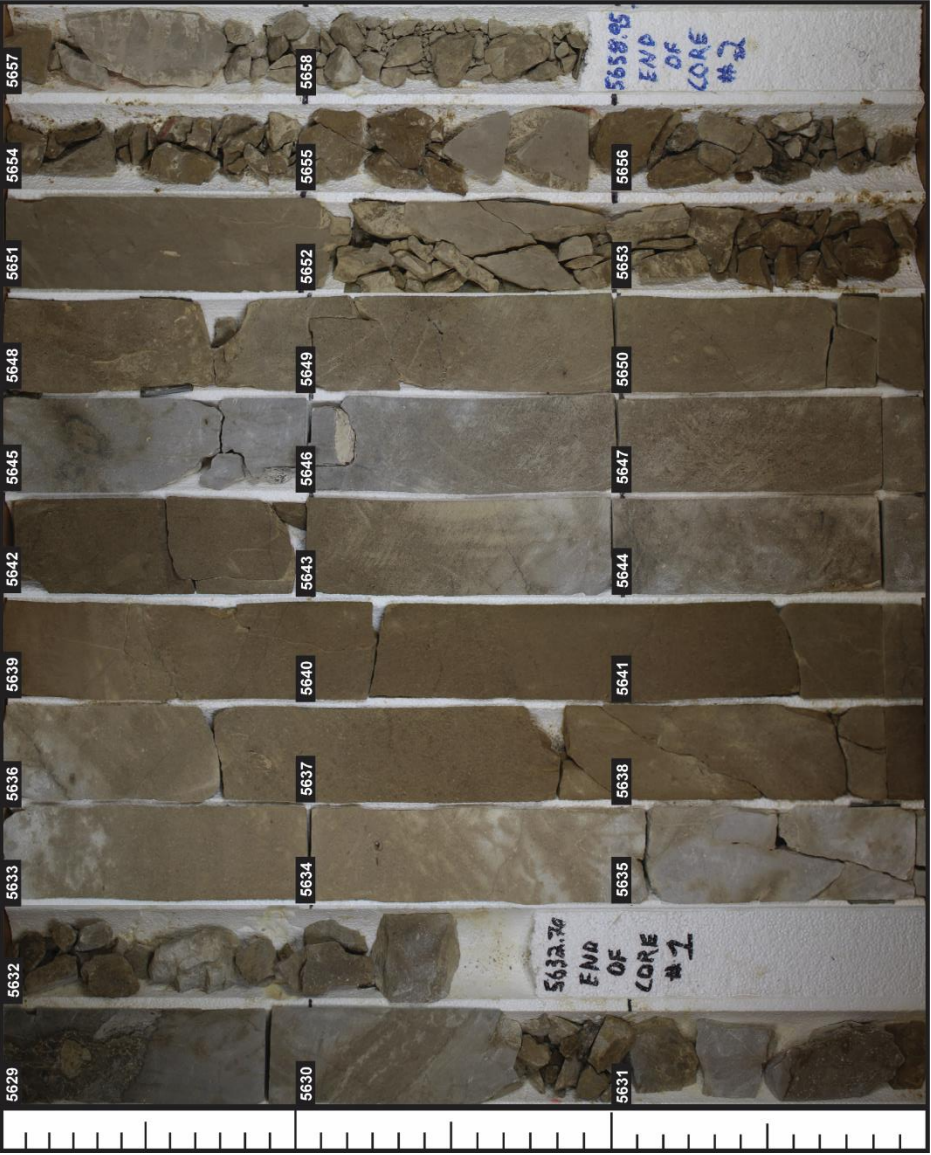


Figure A7. Core image of Simpson Canyon 1044 interval 5629' to 5658.95'.



Figure A8. Core image of Simpson Canyon 1046 interval 5310' to 5355'.

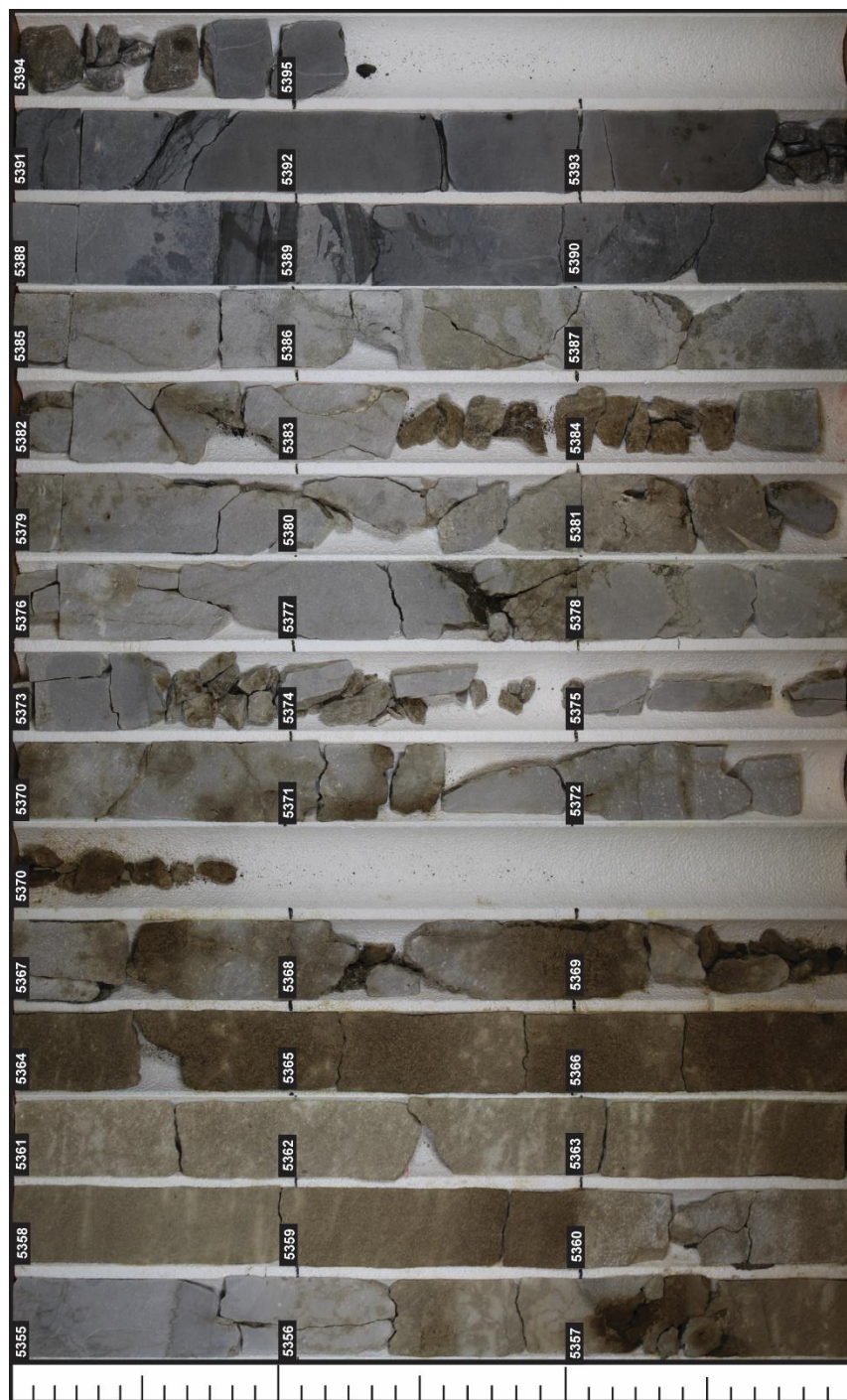


Figure A9. Core image of Simpson Canyon 1046 interval 5355' to 5395.2'.

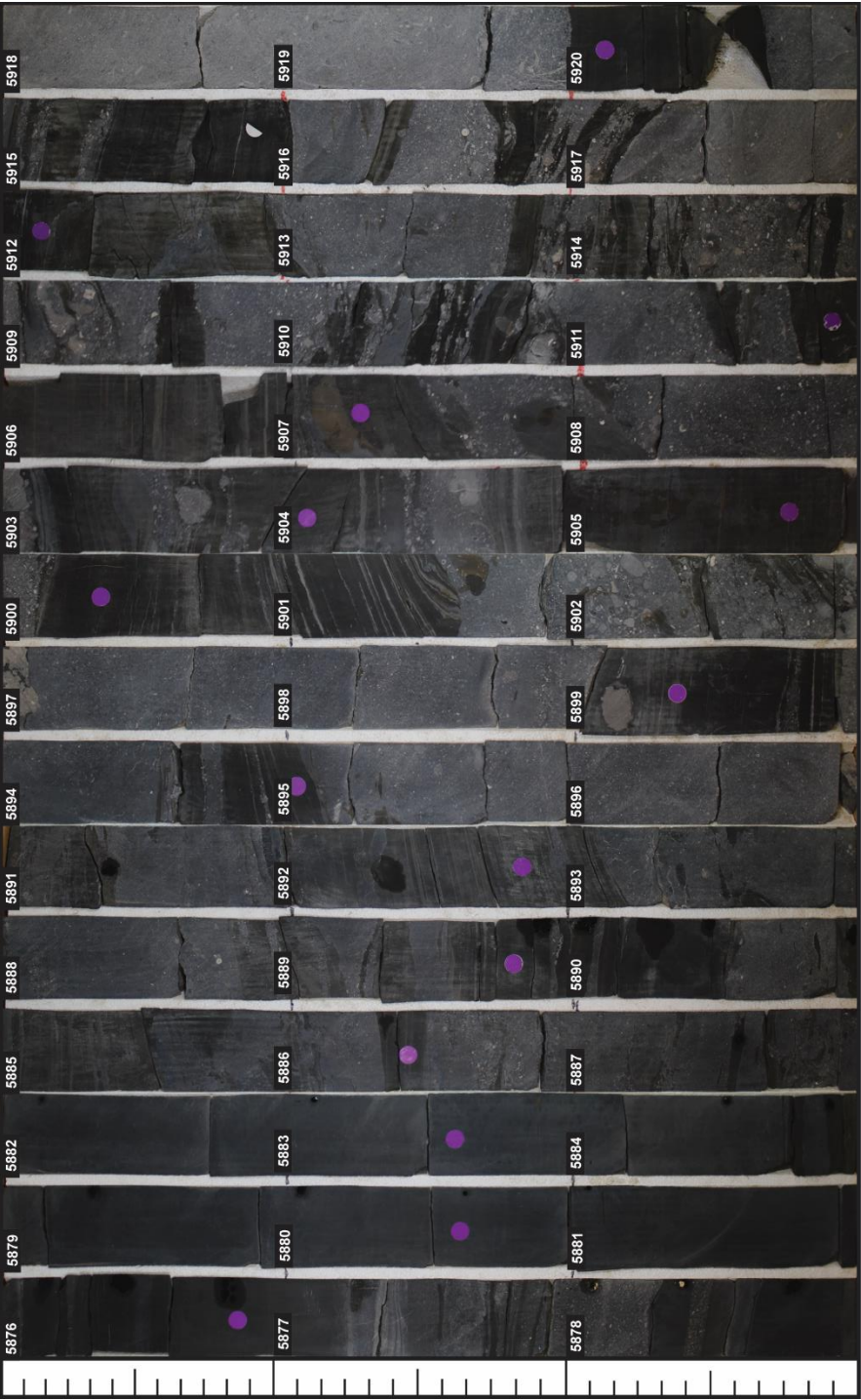


Figure A10. Core image of Simpson Canyon 4045 interval 5876' to 5921'.



Figure A11. Core image of Simpson Canyon 4045 interval 5921' to 5964'.



Figure A12. Core image of Simpson Canyon 4045 interval 5964' to 5996.6'.

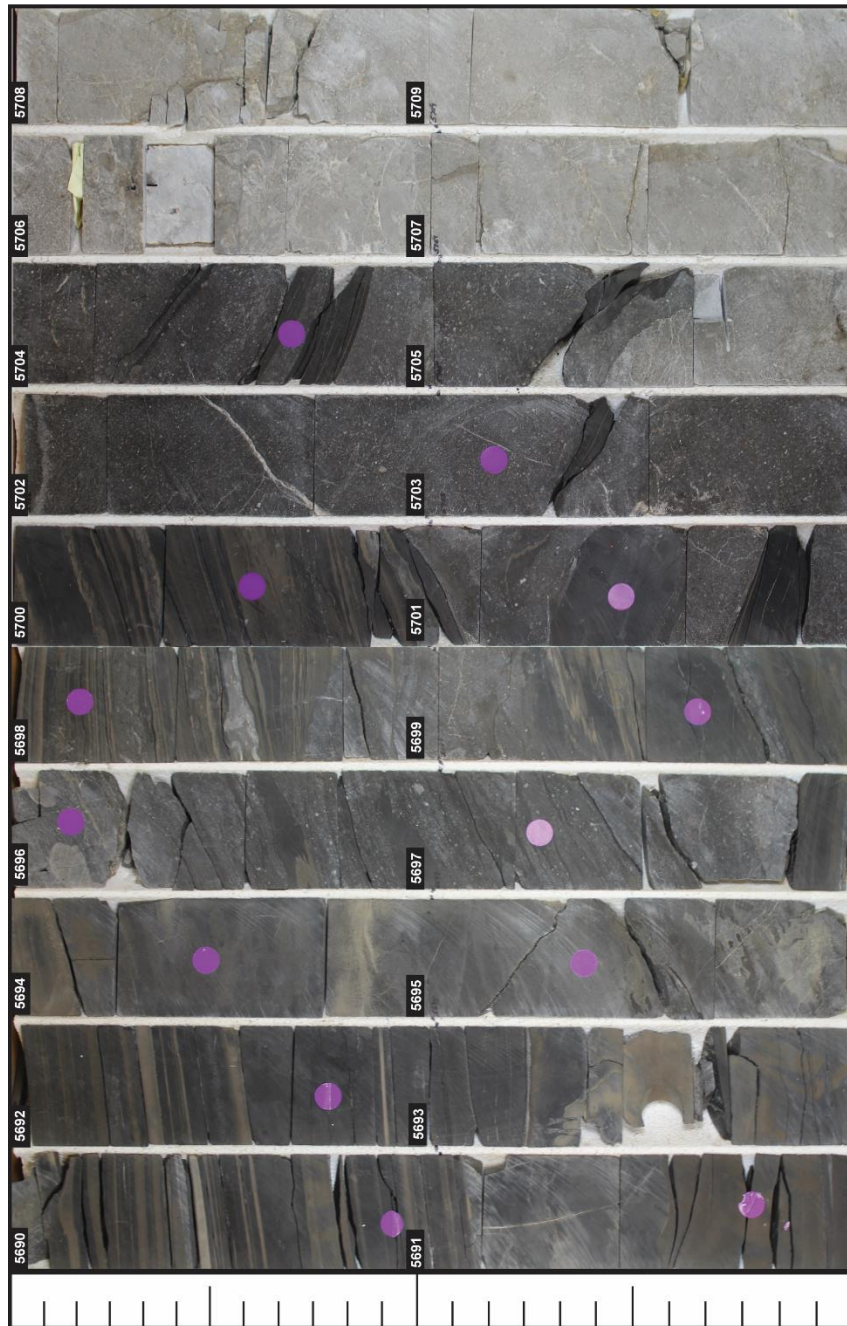


Figure A13. Core image of Simpson Canyon 5027 interval 5690' to 5710'.

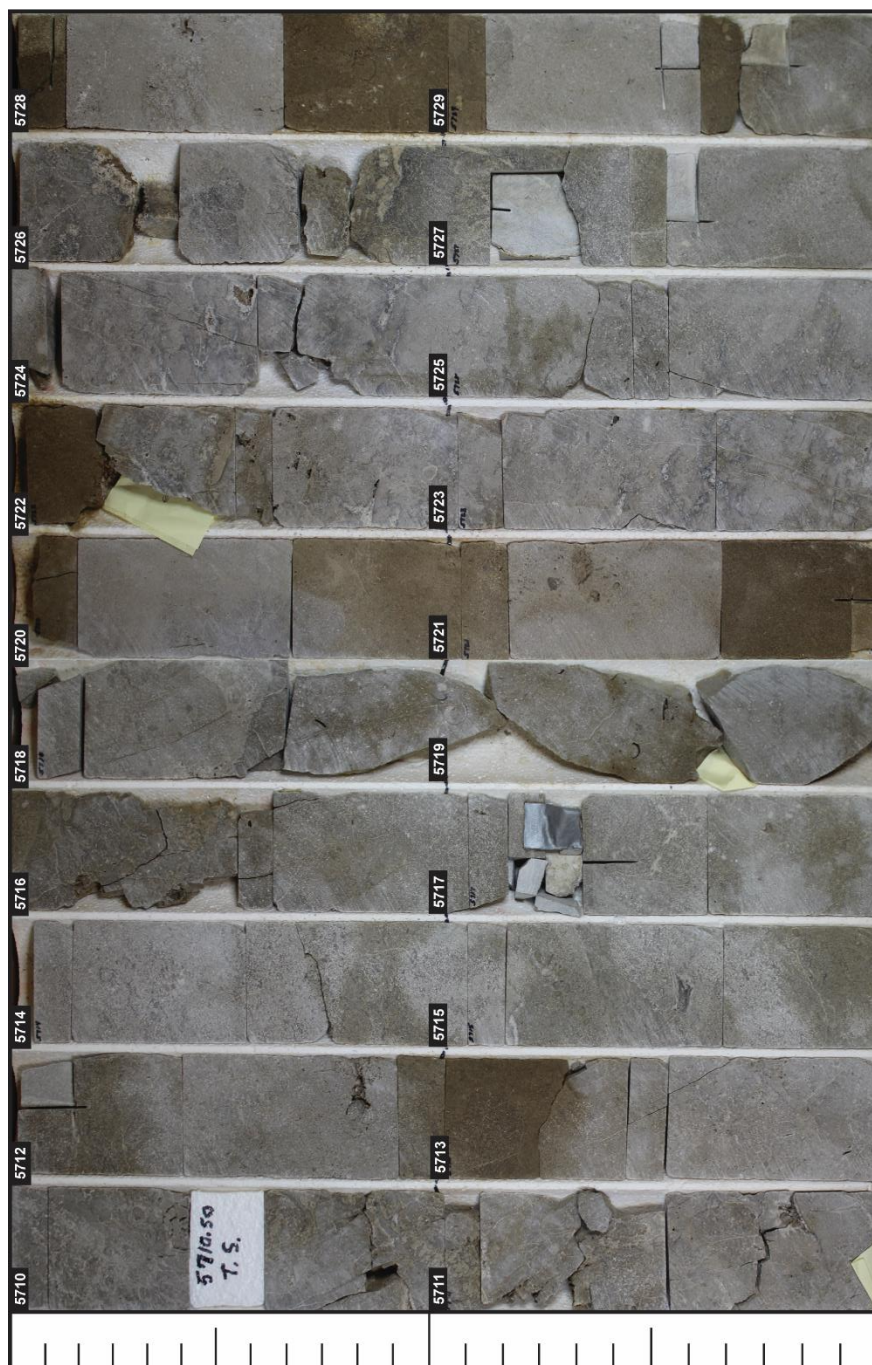


Figure A14. Core image of Simpson Canyon 5027 interval 5710' to 5730'.

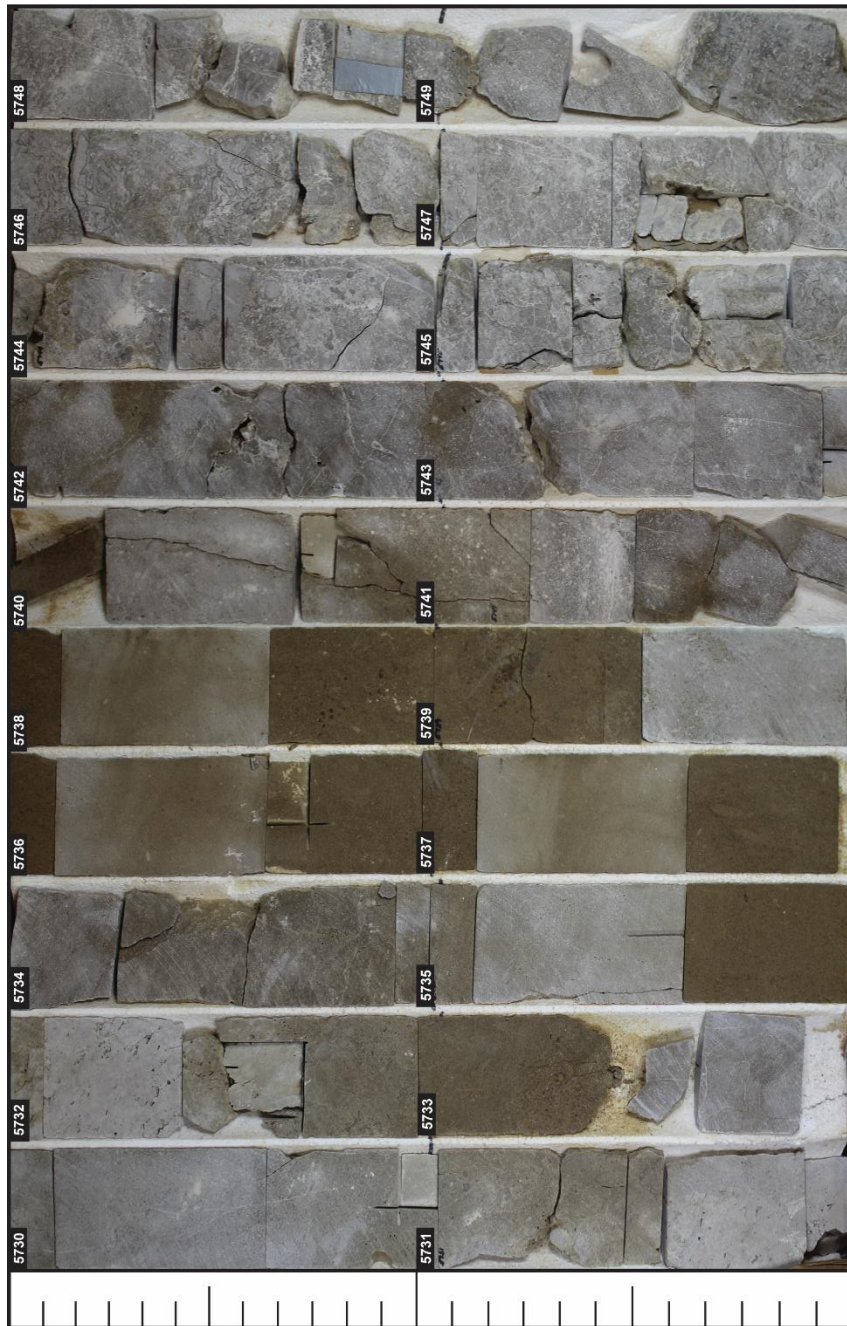


Figure A15. Core image of Simpson Canyon 5027 interval 5730' to 5750'.

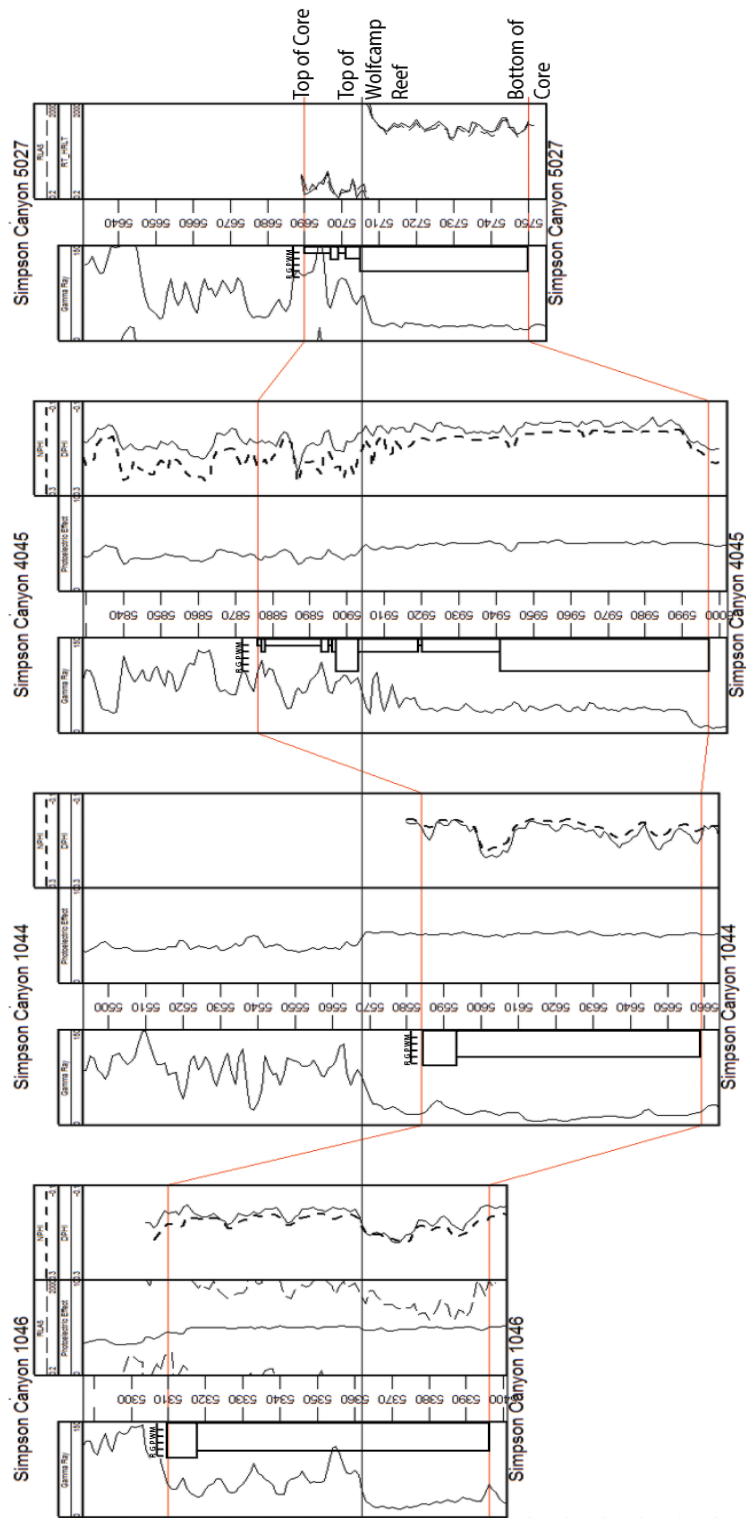


Figure A16. Relationship of wells with the top of the Wolfcamp Reef as a datum and the top and bottom of available cores in red. Simplified lithologies alongside gamma ray logs: (M) Mudstones, (W) Wackestones, (P) Packstones, (G) Grainstones, and (R) Rudstones.

VITA

After completing his work at Henderson High School, Henderson, Texas, in 2006, Wesley Turner attended Kilgore Junior College in Kilgore, Texas, where he found his interest in geology. Afterwards, he attended Stephen F. Austin State University where he graduated with a Bachelor of Science in May of 2013. Afterwards, he continued his education in geology by pursuing a graduate degree at Stephen F. Austin State University and received his degree of Master of Science in May of 2016. At the age of 30, he was last seen diving into a volcano, never to be seen again.

Permanent Address: 210 College ave
Henderson, TX 75654

Style manual designation: Geologic Society of America (GSA)

This thesis was typed by Wesley Luke Turner.